Results from measurements on two insulated solar walls

Søren Østergaard Jensen

THERMAL INSULATION LABORATORY
TECHNICAL UNIVERSITY OF DENMARK
REPORT NO. 247   MARCH 1993

Project group

Experiment:

Lars Olsen, MSc, PhD
Flemming Karn, technician
Bertil Morelli, technician

Report:

Søren Østergaard Jensen, MSc

Preface

The present report concludes the project "Solar walls phase II" financed by the Danish Ministry of Energy - journal no 1353/85-5. The preceding project "Solar walls phase I" is reported in ref. [1].

The experiment reported in the report was carried out during the first five months of 1986, while the results from the experiment were reported by the end of 1992-beginning of 1993. The results from the experiment were further reported by a person, who did not participate in the planning or execution of the experiment. This may be the reason for inconsistencies (if any) in the report.

Summary

The present report describes the findings from an experiment with two heavy mass solar walls. For both solar walls different measures were taken in order to decrease the heat loss from the mass component through the cover.

In the first wall a vertical blind of bright plastic foil was installed between the cover and the mass component. The blind was turnable and operated in such a way that during the day the slats of the blind were always parallel with the solar beams and during the night they were closed in order to decrease the radiative and convective losses through the cover.

The second wall was an internally ventilated Trombe wall. An insulating panel was mounted in the space between the mass component and the absorber. A transparent cover was further installed in front of the absorber. The two air gaps on each side of the insulating panel were connected by an opening at the top and at the bottom of the insulating panel. The heat absorbed by the absorber was transported to the mass component by a thermosiphonic air stream between the two air gaps on each side of the insulating panel. In order to prevent a reverse air circulation, dampers were mounted in the openings at the top and bottom of the insulating panel. The dampers were made of plastic foil and metal grids.

The report describes the results obtained from measurements from two measuring periods in the beginning of 1986. Different temperatures of the walls are shown. The U-values, the overall net heat gains and the solar gains of the walls have been calculated. The thermal comfort of rooms with the walls are furthermore discussed and it is described how overheating problems may be reduced.

It is estimated that the walls are suitable under Danish weather conditions. More detailed investigations are, however, necessary in order to determine the annual savings of the walls installed in real buildings and in order to investigate if the walls are profitable.

Table of Contents

1 Introduction

There has been a growing interest in utilizing the sun for heating purposes during the last decades because of an increasing understanding of the environmental problems when using fossil fuels. Passive solar heating is one way to utilize the solar radiation.

A solar wall is a passive device for utilization of the solar radiation on the thermal envelope of a building. The most simple solar wall consists of a massive wall which is painted black on the outside. In order to decrease the heat loss to the ambient a transparent cover is mounted in front of the wall. When the solar radiation hits the black painted wall, the wall will be heated up. Some of the heat will, by conduction, be transported to the room behind the wall. Depending on the heat capacity and thermal conductivity of the massive wall the transport of solar heat will be delayed and the massive wall will act as a thermal storage. The heat gained by the solar wall will thus be in less conflict with the direct solar gain through the windows of the building.

Several different kinds of solar walls exist, suited for different climates and different purposes. Under Danish weather conditions it is necessary to use well insulated solar walls in order not to lose too much of the collected solar energy to the environment and to minimize the heat losses in periods with no solar radiation.

The present report describes the results obtained from an experiment with two insulated solar walls. The design of the solar walls was based on earlier experience - theoretical considerations, simulations and experiments (ref. [1]). For both walls special measures were taken in order to decrease the heat loss through the cover.

In the first wall a vertical turnable blind was installed between the mass component and the cover. The blind was made of bright plastic foil. The blind was operated in such a way, that the slats of the blind were always parallel with the solar beams during the day, while the blind was closed during the night. Due to the bright surfaces of the blind the radiative heat loss was descreased during the night, but also during the day. The convective heat loss was also decreased. The blind did, however, also cut off some of the diffuse solar radiation.

For the second solar wall another concept was chosen. The wall was an internally ventilated Trombe wall. The principles of the wall are shown in fig. 1.1. The principles of the wall are, that an insulated panel is installed between the mass component and the absorber. The heat from the absorber is transported to the mass component by means of a thermosiphon air stream. Two plastic foils (dampers) were mounted at the top and bottom air gap of the insulating panel in order to prevent a reverse circulation during the night which would discharge the mass component heat storage.

The solar walls and the test are described in detail in the following chapter.

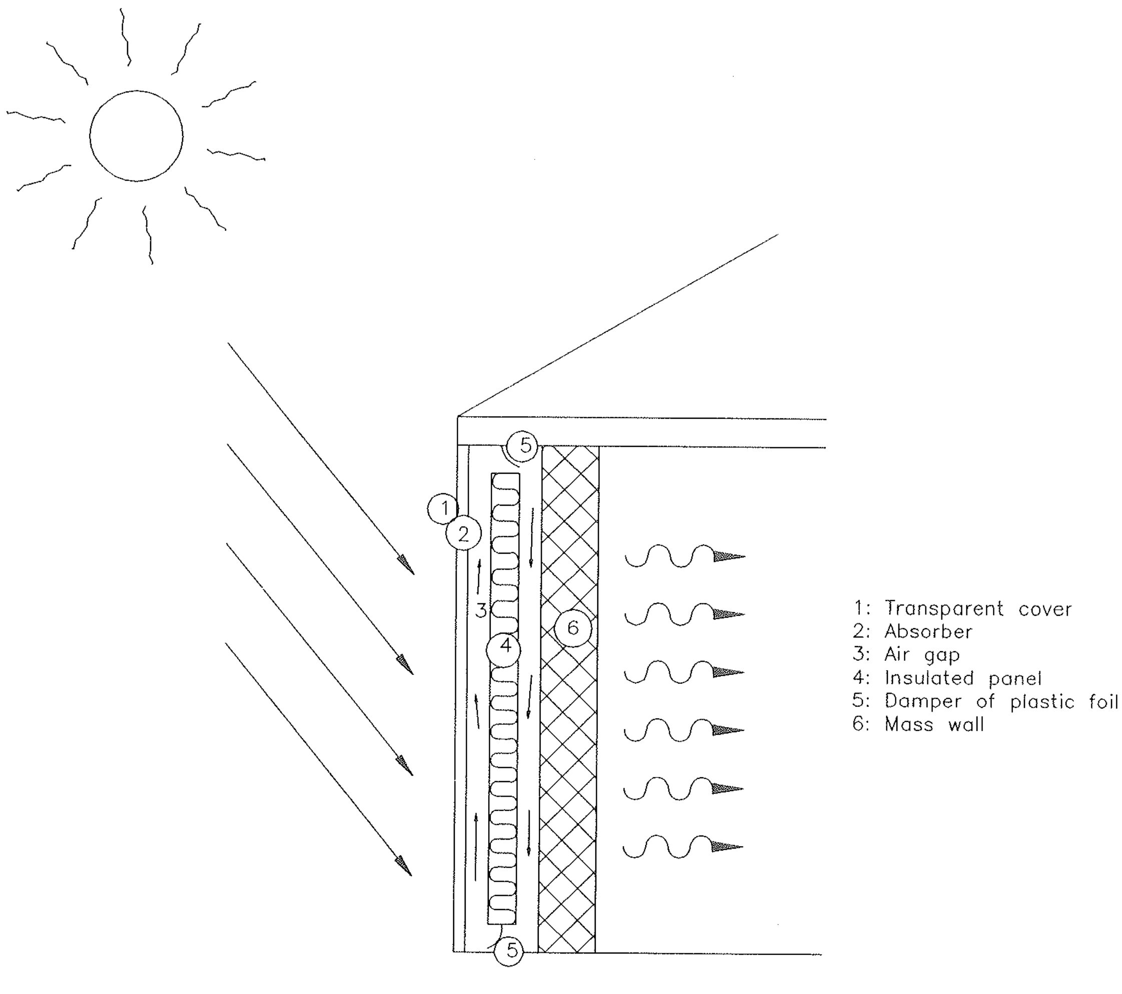

Figure 1.1 The principle of the second solar wall - an internally ventilated Trombe wall.

2 Description of the experiment with the solar walls

The present chapter describes the two solar walls and the experiment.

2.1 The experimental building

The two solar walls were tested in an experimental building at the campus of the Technical University of Denmark. Figure 2.1 shows the layout of the experimental building while fig. 2.2 shows the two solar walls mounted in the south facade of the experimental building.

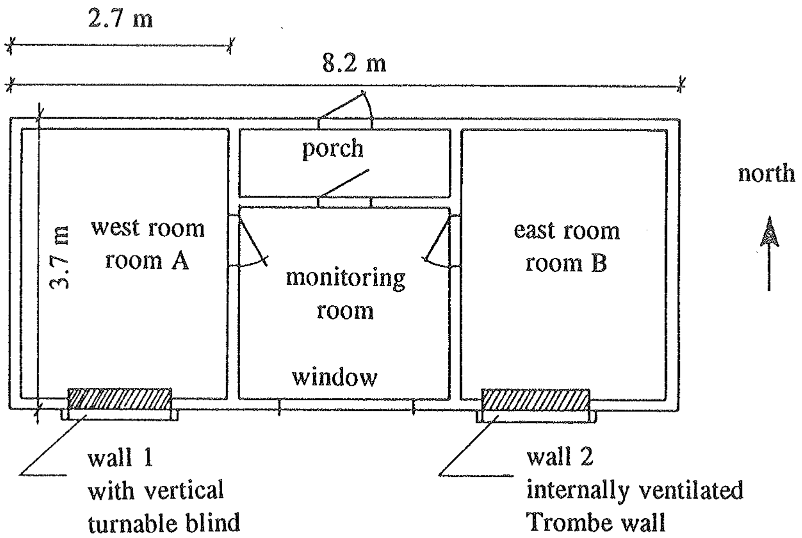

Figure 2.1 Layout of the experimental house where the two solar walls were tested.

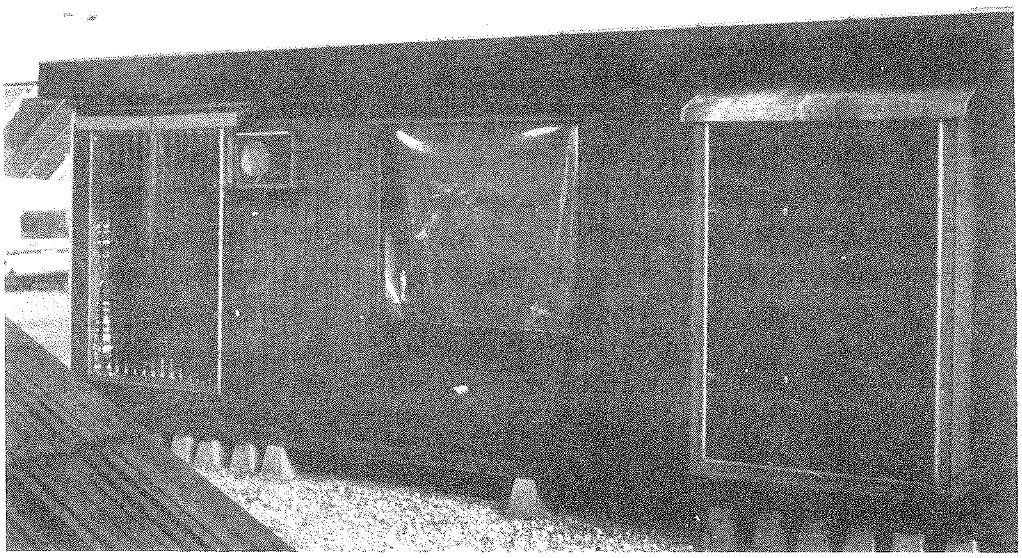

Figure 2.2 The two solar walls mounted in the experimental building. The solar wall with the vertical turnable blind is the one to the left, while the internally ventilated Trombe wall is to the right.

The experimental building consisted of two identical test rooms and between them a room for measuring equipment and a porch. The construction of the experimental building was wooden beams and laths with the outer walls, floor and roof insulated with 100 mm mineral wool (ref. [2]). White screens were mounted on the east and west facades with a ventilated air gap between the screens and the facades in order to reduce the influence of the solar radiation on these facades. The inner surfaces of the walls (except for the solar walls) consisted of plywood, while the floor was made of chipboard and the ceiling of gypsum plates. The floor area of the test rooms was 10 m^2. Auxiliary heat was supplied by thermostatically controlled electric panels in order to maintain the room temperature level at approximately 20°C.

The mass component of the solar walls consisted of sand/lime bricks with the following properties:

Thermal conductivity	0.95 W/mK
Density	1800 kg/m
Specific heat	800 J/kgK

Table 2.1 The thermo-physical properties of the mass component. The properties are taken from handbooks - not measured for the actual materials.

A vertical section of the mass component is shown in fig. 2.3. The thickness of the walls were 0.228 m. Figure 2.4 shows one of the mass components before the rest of the solar wall was installed. Figure 2.5 shows a close-up of the mass component. A more detailed description of the mass components can be found in ref. [1].

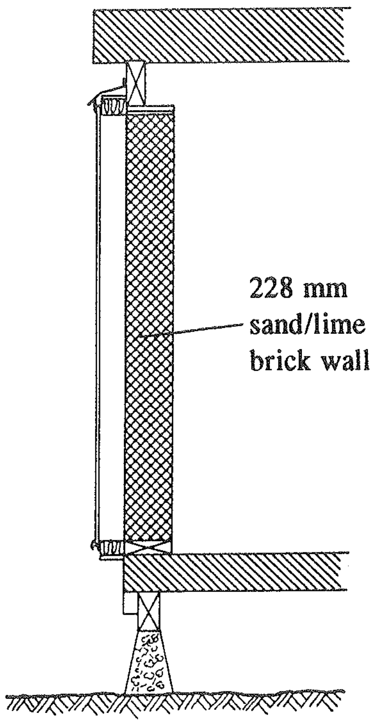

Figure 2.3 Section of one of the mass components.

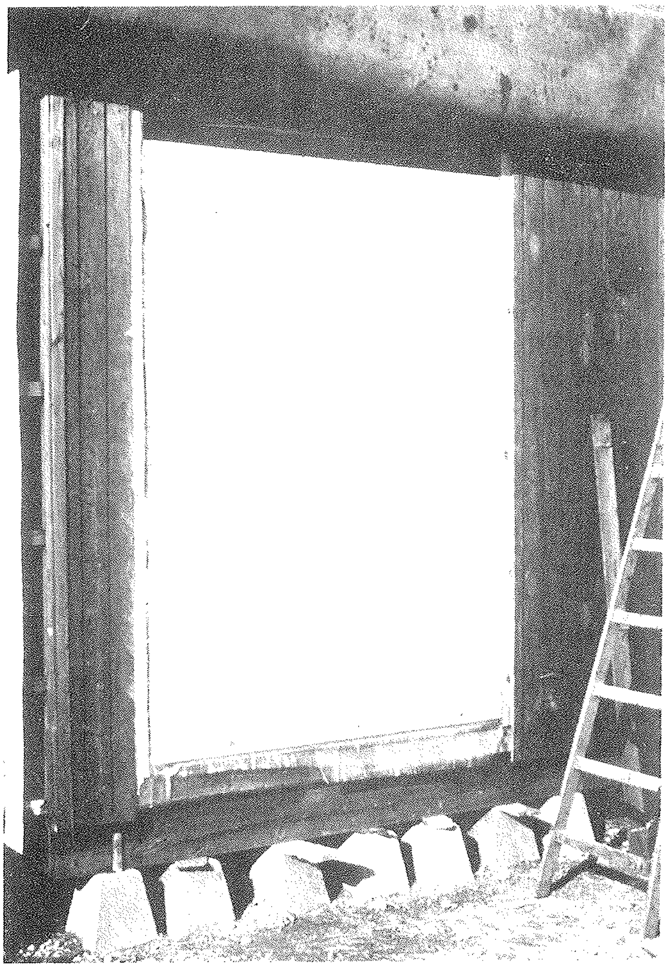

Figure 2.4 The mass component before installation of the rest of the solar wall.

Figure 2.5 Close-up of the mass component.

Figure 2.6 shows the overall dimensions of the solar walls and the dimensions of the transparent area. The numbers in brackets are the dimensions of the internally ventilated Trombe wall.

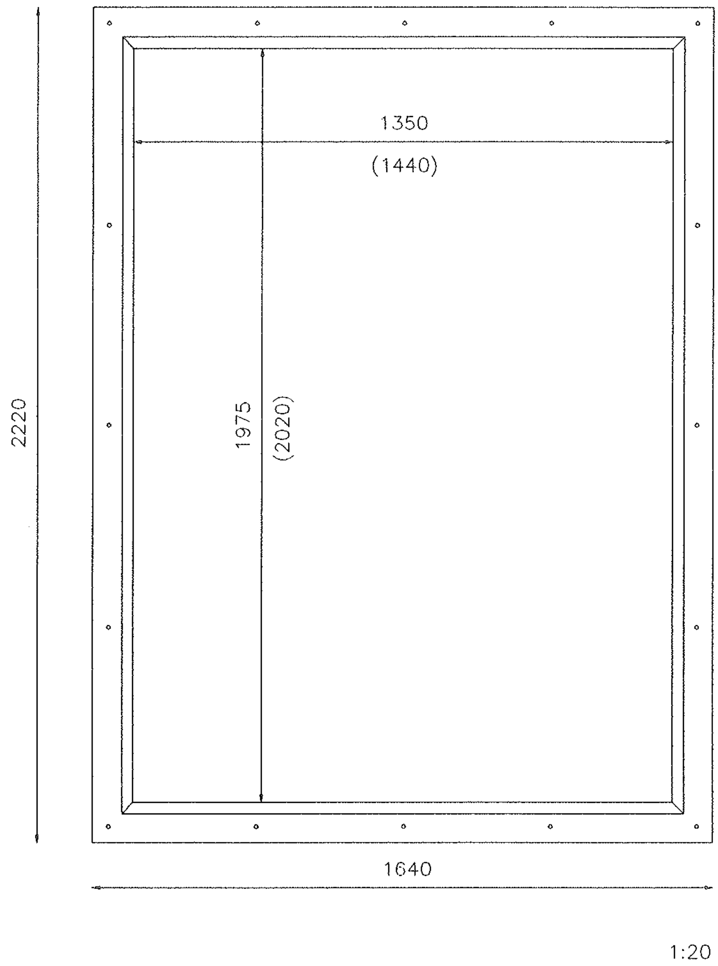

Figure 2.6 The overall dimensions of the solar walls and the dimensions of the transparent area, all in mm.

2.2 Solar wall no 1: with vertical turnable blind

The solar wall was, as already mentioned, equipped with a vertical turnable blind between the mass component and the cover. The cover consisted of 5 mm ordinary glass. The transparent area of the solar wall was approximately 2.91 m^2. Selective foil (Maxorb) was fastened to the outer surface of the mass component in order to reduce the radiative heat loss from the solar wall further. Figure 2.7 shows the solar wall. The wheel at the top right corner of the solar wall was for operating the blind. The wheel was connected to a damper motor and a timer. The blind was operated in such a way, that the slats of the blind were always parallel to the solar beams during the day and closed during the night. Figure 2.8 shows the traverse rod for turning the blind.

Figure 2.7 Photograph of the solar wall with the blind.

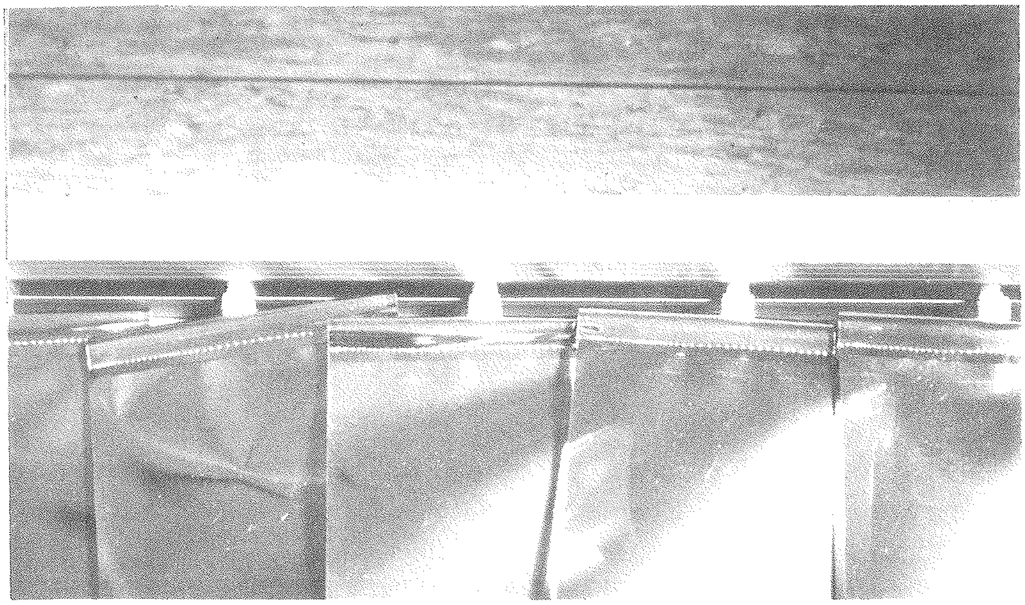

Figure 2.8 The traverse rod for turning the blind.

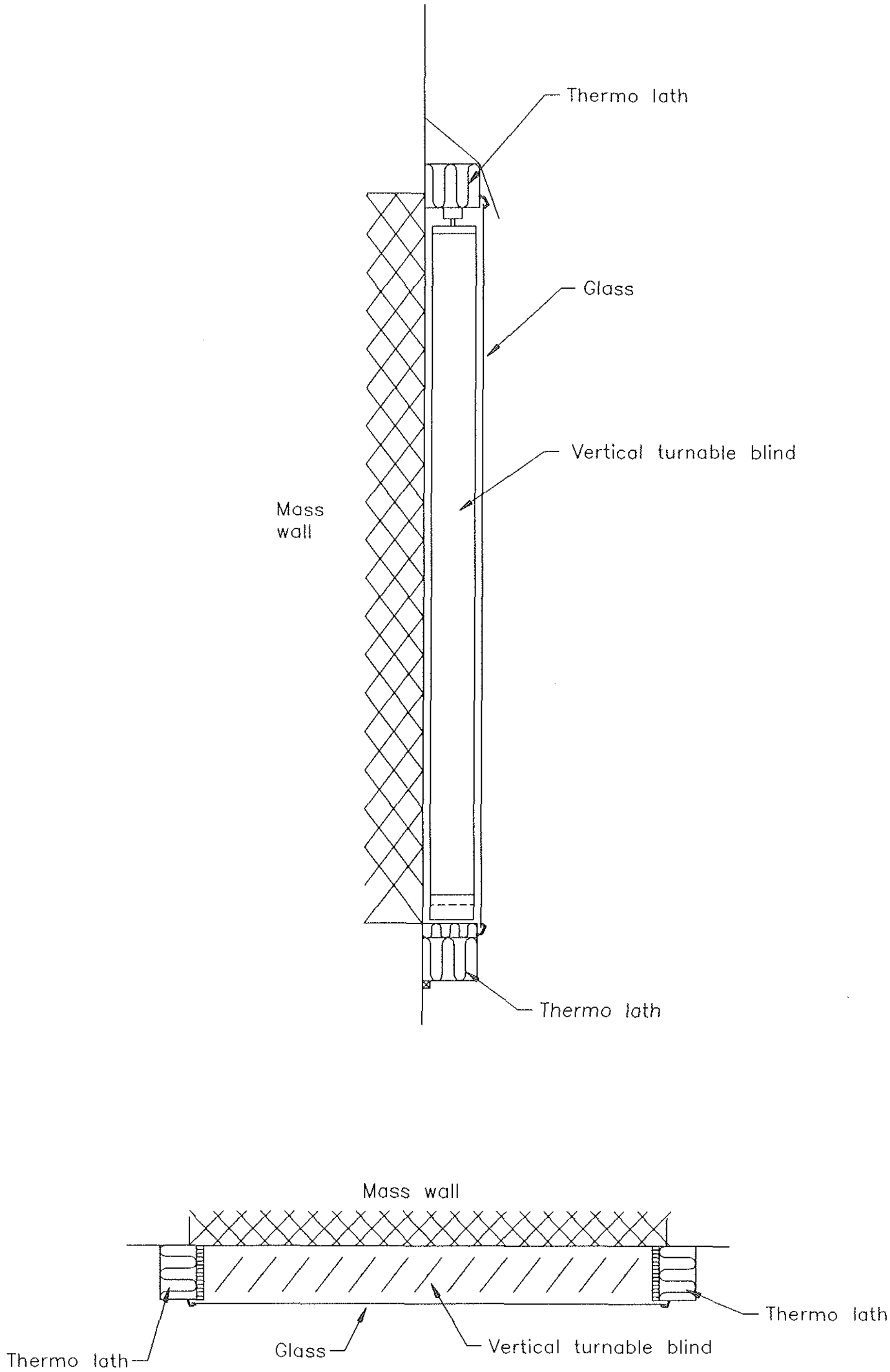

Figure 2.9 The overall design of the solar wall with the blind.

Figures 2.9-12 show in detail the design of the solar wall with the blind. Thermo laths were mounted around the solar wall in order to reduce uncontrolable heat losses and thermal bridges. The dimensions of the cross section of the thermo laths are given in fig. 2.10. The thermo laths were made of plywood and small wooden laths and filled with soft mineral wool. Additional 15 mm hard mineral wool was mounted on the inner surface of the side thermo laths and 30 mm on the inner surface of the bottom thermo lath. Bright adhesive plastic foil was fastened to the additional hard insulation in order to reflect the solar radiation on the thermo lath to the absorber on the mass wall.

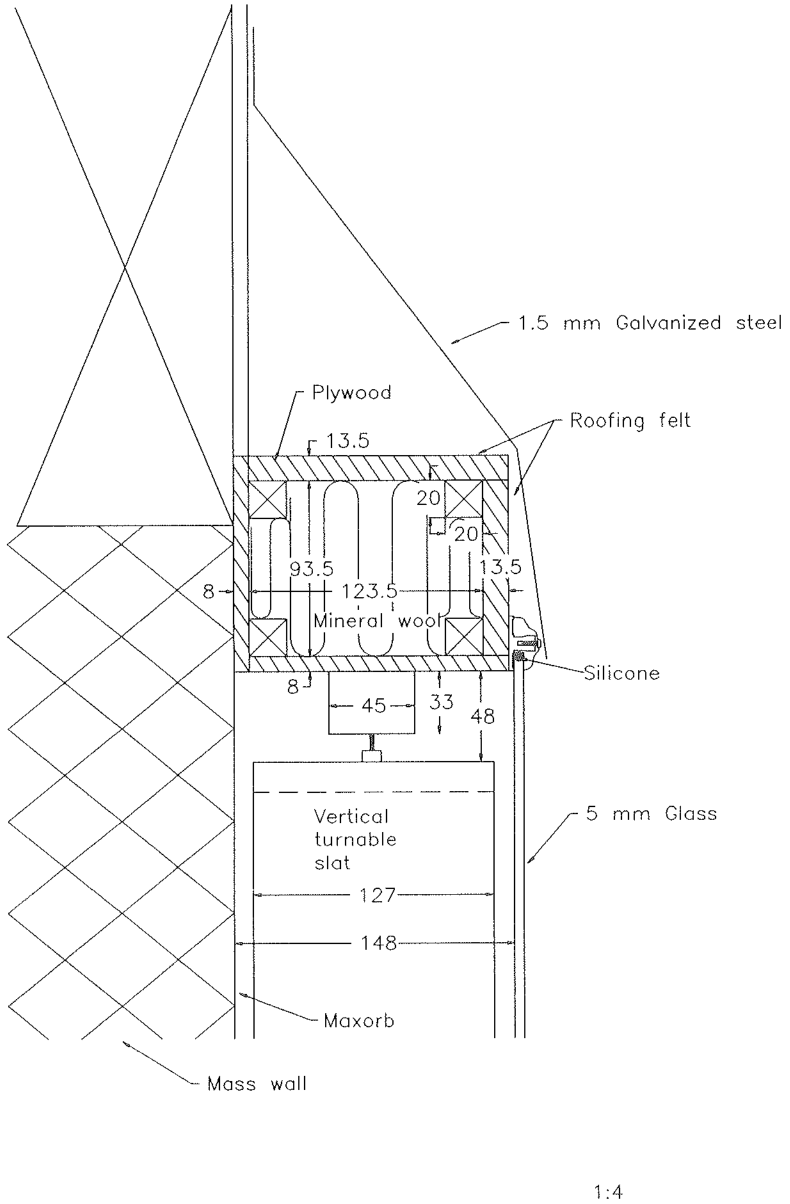

Figure 2.10 Vertical section. Details of the top of the solar wall with the blind.

The solar wall consists counted from the outside of a 5 mm cover of ordinary glass fastened to the thermo laths by means of aluminium profiles and sealing strips. A vertical and turnable blind was mounted in the 148 mm air space between the cover and the mass wall. The surface of the mass wall was covered by a selective foil - Maxorb foil.

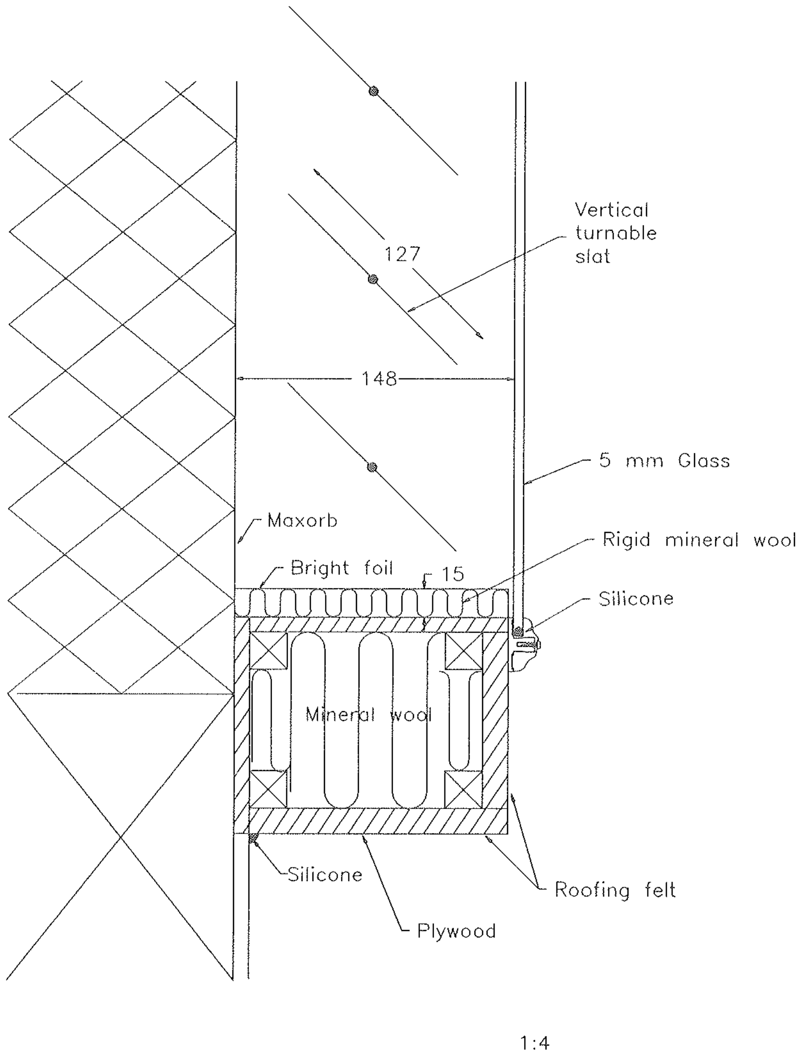

Figure 2.11 Horizontal section. Details of the side of the solar wall with the blind.

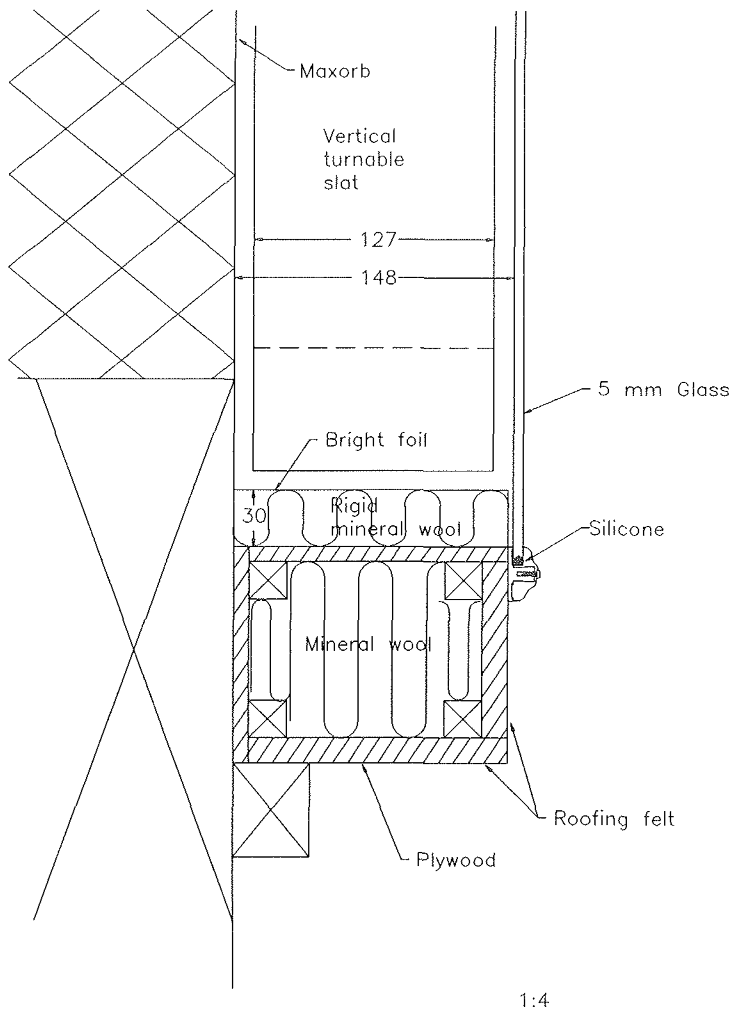

Figure 2.12 Vertical section. Details of the bottom of the solar wall with the blind.

2.3 Solar wall no 2: internally ventilated Trombe wall

The solar wall had an insulating panel between the mass component and the absorber. A transparent cover of 5 mm ordinary glass was further mounted in front of the absorber. At the top and bottom of the insulating panel were two openings allowing the air to circulate between the two air spaces on each side of the insulating panel. A plastic foil (Teflon) and a grid were mounted in the openings at the top and bottom of the insulating panel. The plastic foil and grid acted as a damper with a built-in non-return valve. The air was thus only allowed to circulate in one direction - up along the back of the absorber and down along the mass component. In this way heat loss by counter-flow during the night was prevented. Figure 2.13 shows a photograph of the solar wall, while figs. 2.14-17 show the design of the wall in detail. Figure 2.18 shows the insulated panel before installation and figs. 2.19-20 show the bottom and top damper, respectively.

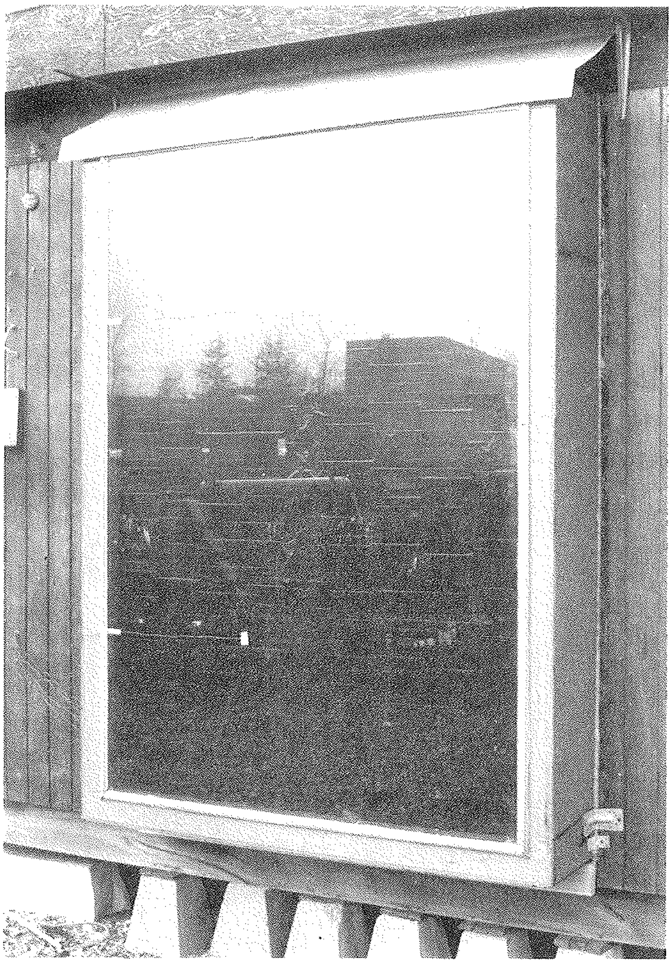

Figure 2.13 Photograph of the internally ventilated Trombe wall.

The solar wall consists named from the outside of a 5 mm cover of ordinary glass fastened to the thermo laths by means of aluminium profiles and sealing strips. The transparent area of the solar wall was approximately 2.67 m^2. The cover was mounted 55 mm in front of the absorber which consisted of 1 mm aluminium with a selective surface - Maxorb foil. Between the absorber and the mass component an insulating component was mounted. The absorber was fastened to the thermo laths by means of wooden laths and aluminium profiles. The absorber was also fastened to the insulating panel in the middle by an aluminium profile - see fig. 2.14. The insulating panel consisted of a wooden framework with soft mineral wool and hard masonite on each side. The wood/mineral wool ratio was 0.13 (corresponding to 11.5 % of the overall area of the wall).

At the top and the bottom of the insulating panel a damper was installed. The two dampers were made of Teflon foil and a metal grid. The Teflon foil was extremely thin which made it possible for the thermosiphon air stream to open the damper during a day with solar radiation. During periods without solar radiation the air will tend to circulate the opposite way around and thereby discharge the storage to the surroundings. This reverse flow was prevented by the grid, as the Teflon foil was sucked tight to the grid and thereby closing the opening. The

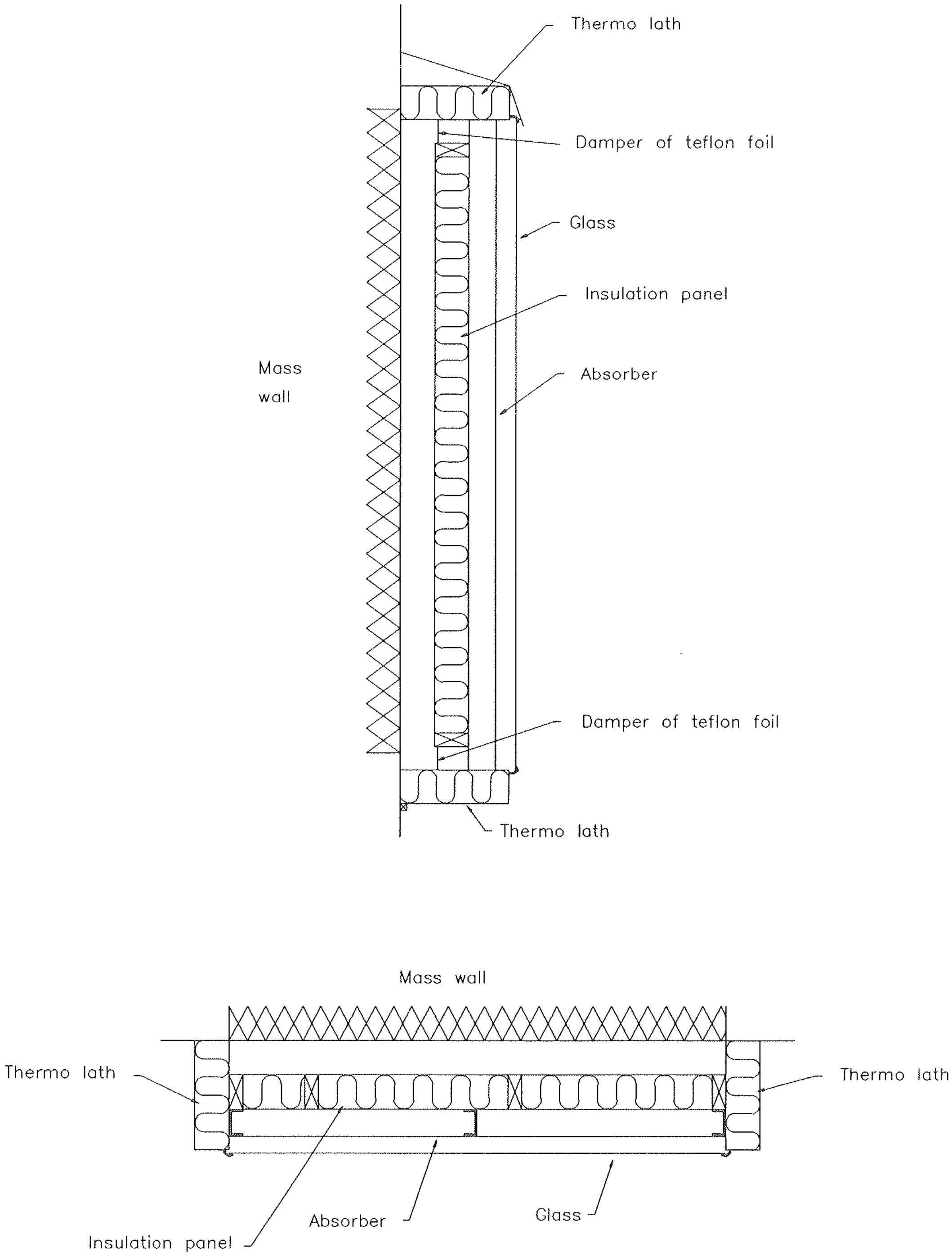

Figure 2.14 The overall design of the internally ventilated Trombe wall.

opening area of the top damper was approximately 0.115 m^2, while the opening area of the bottom damper was approximately 0.138 m^2. The cross section of the external air gap was approximately 0.108 m^2 and the cross section of the air gap between the insulating panel and the mass component was approximately 0.132 m^2.

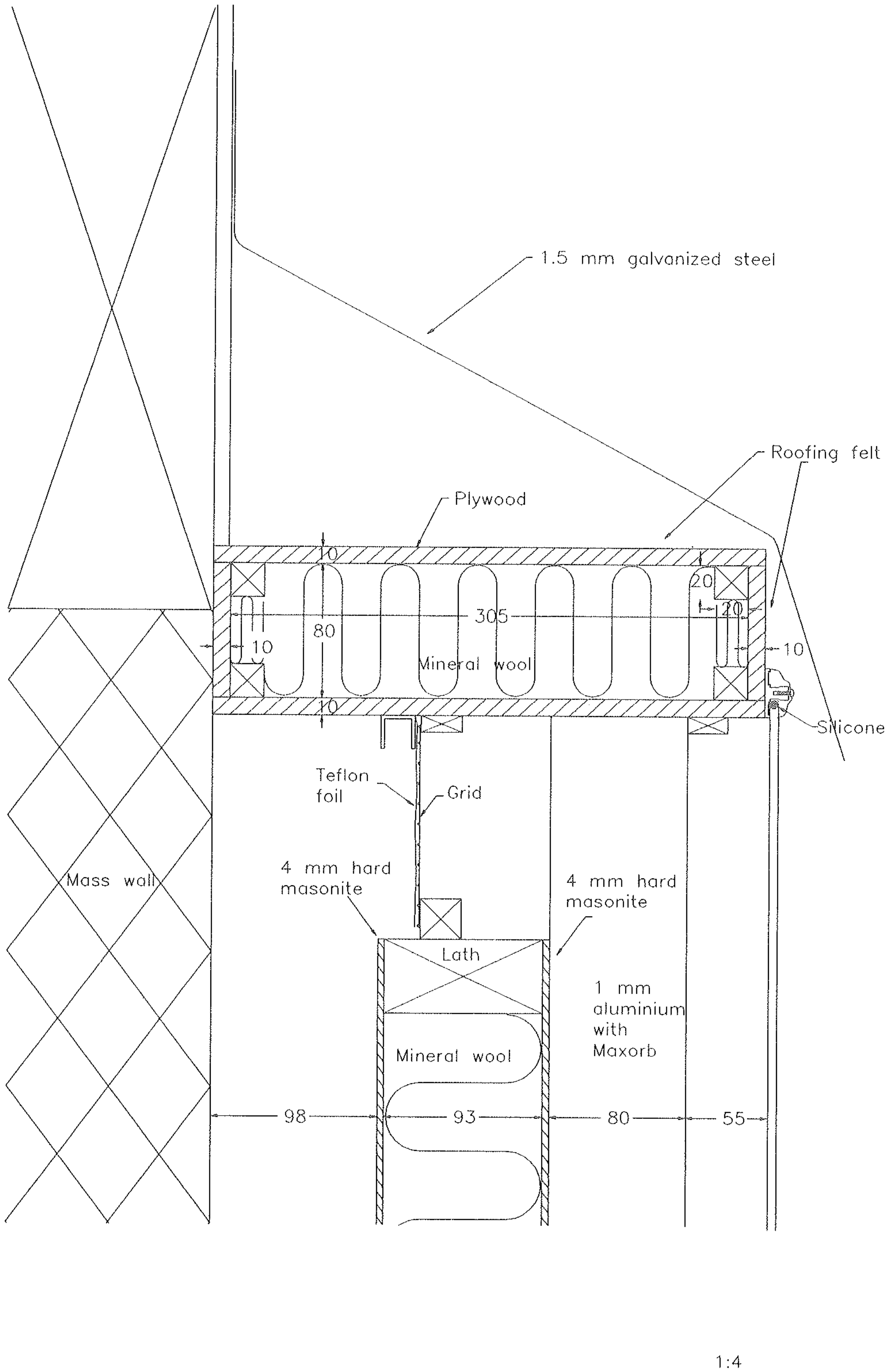

Figure 2.15 Vertical section. Details of the top of the internally ventilated Trombe wall.

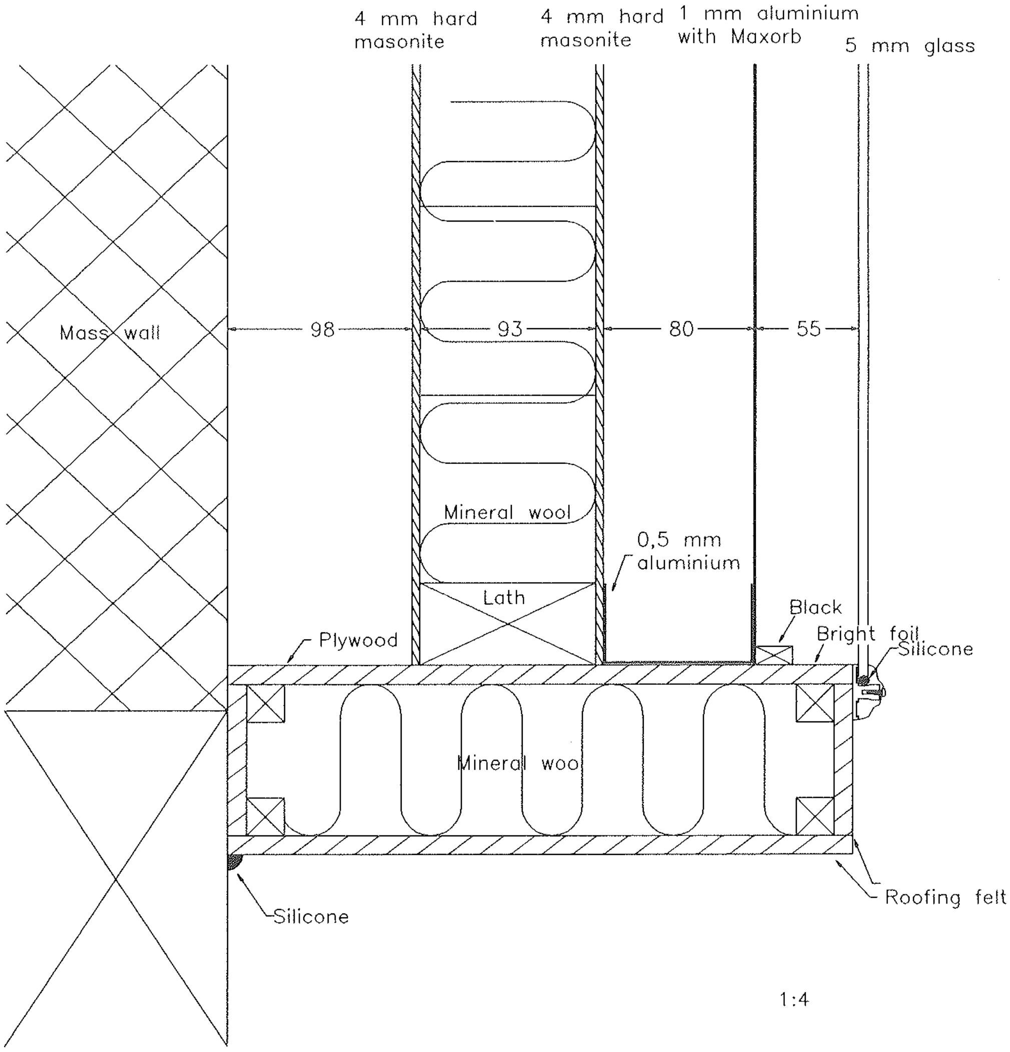

Figure 2.16 Horizontal section. Details of the side of the internally ventilated Trombe wall.

Bright adhesive plastic foil was mounted on each of the side thermo laths and the bottom thermo lath between the cover and the absorber - see figs. 2.16-17. Most of the solar radiation on these areas was, therefore, reflected to the absorber.

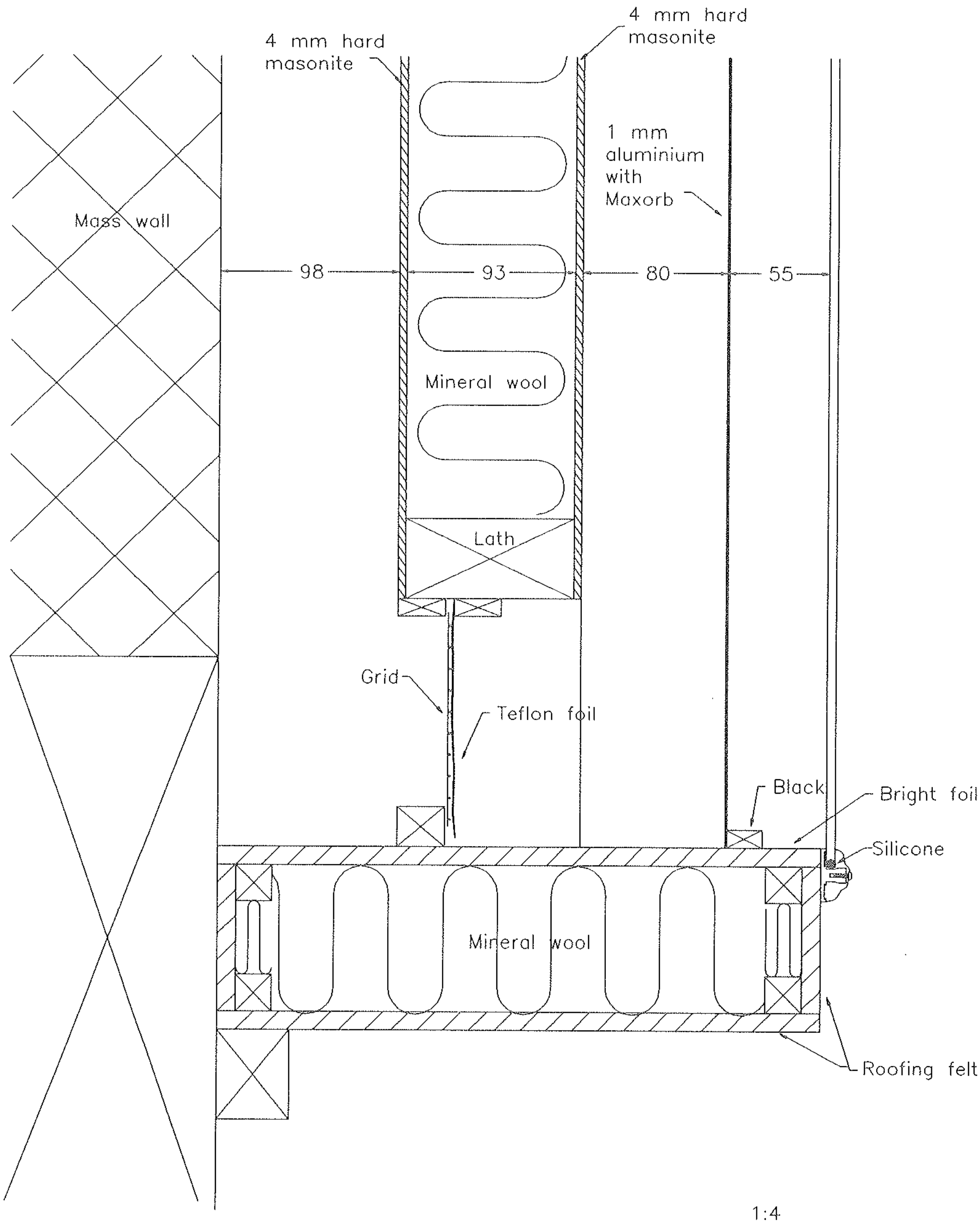

Figure 2.17 Vertical section. Details of the bottom of the internally ventilated Trombe wall.

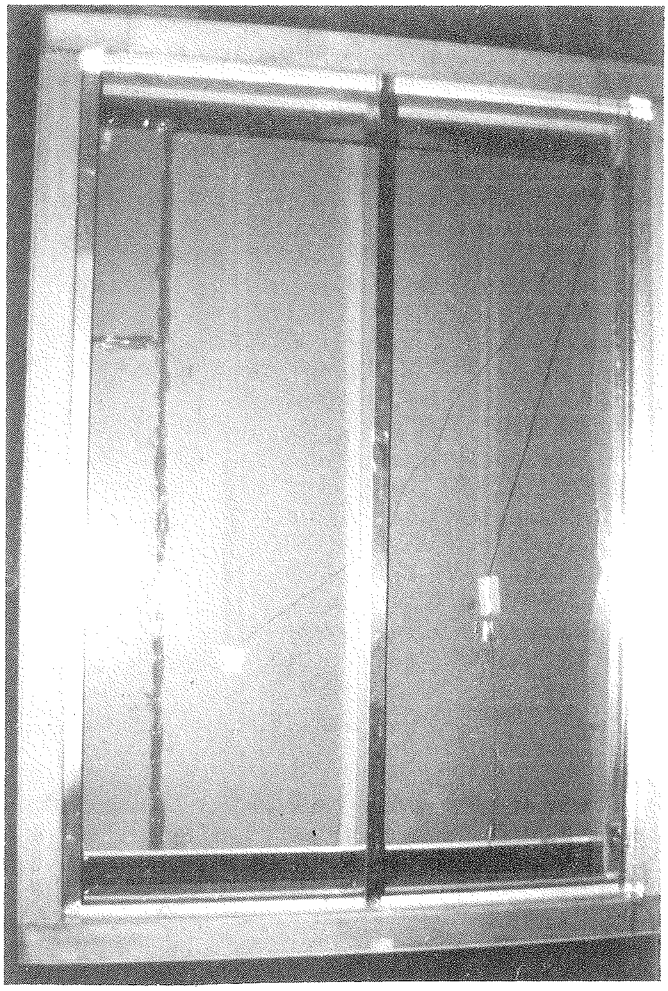

Figure 2.18 The insulating panel of the internally ventilated Trombe wall (before the absorber was mounted). Note the spacing profiles of aluminium (vertical - on both sides and in the middle) for maintaining the distance between the absorber and the insulating panel.

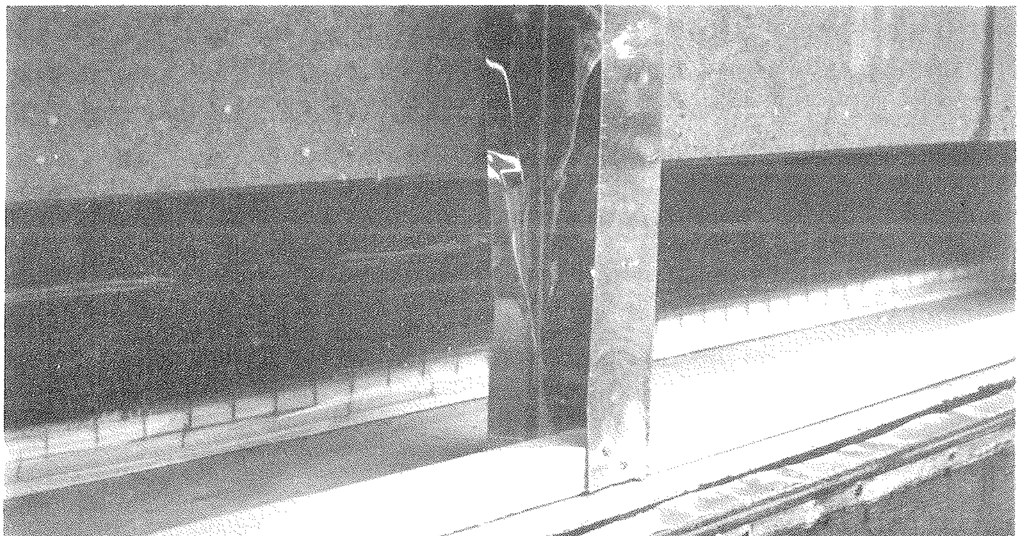

Figure 2.19 Bottom damper of the internally ventilated Trombe wall. Note the aluminium profile and lath to keep the absorber plane.

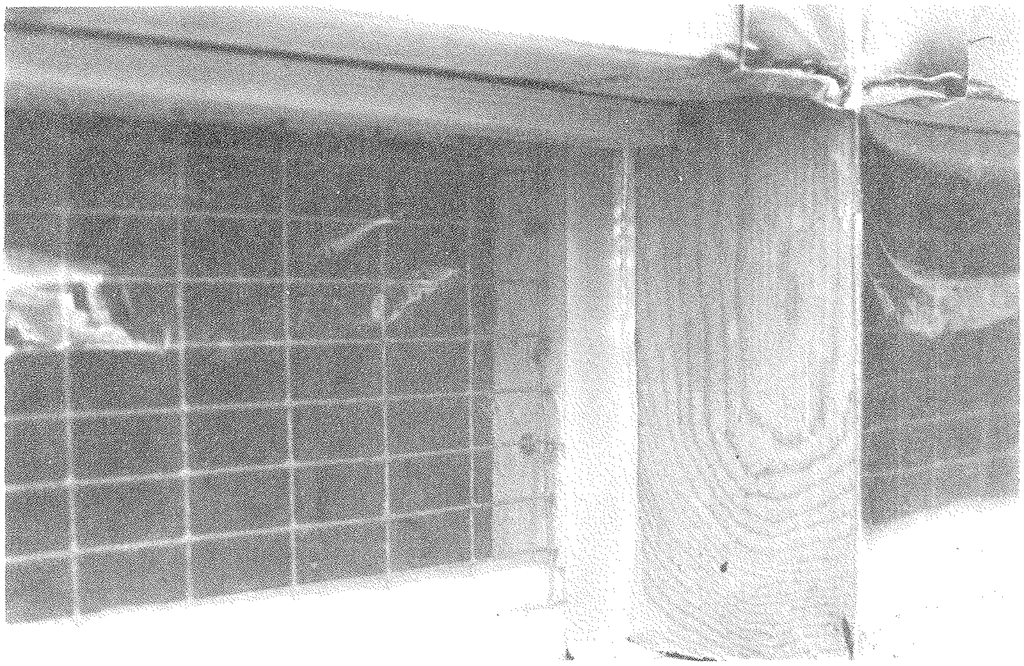

Figure 2.20 Top damper of the internally ventilated Trombe wall. Note the grid and the Teflon foil.

2.4 The measuring system

In this section the applied measuring system will briefly be described. Further details can be found in ref. [1] and [3].

27 measuring points were scanned every 10 minutes and stored on tape for further analyses. The measuring points are listed in table 2.2.

The position of the measuring points of the mass components are given in fig. 2.21. The temperatures of the mass walls were, for wall 1, mean values of 5 thermocouples (connected as thermopiles) as shown in the left part of fig. 2.21, while for wall 2 the thermocouples at the middle of the wall were disconnected.

The measuring of the surface temperatures of the rooms was performed with thermopiles with 14 elements mounted on the floor, ceiling and walls except for the mass wall.

The measuring of the heat flow through the internal surface of the mass walls was performed with heat flow meters with 80 junctions - see ref. [1] and [3] for further details.

The rest of the temperatures were measured with thermopiles with several elements or only with thermocouples - see table 2.2.

The ambient temperature was measured with a shielded thermocouple on the north side of the experimental building. The pyranometers for measuring the total and diffuse radiation at vertical south and the cup anemometer for measuring the wind speed along the south facade are shown in fig. 2.22.

Wall no	Measuring point	Unit	*
1	Temperature of the mass wall (position A)**	°C	5
1	Temperature of the mass wall (position B)**	°C	5
1	Temperature of the mass wall (position C)**	°C	5
1	Temperature of the mass wall (position D)**	°C	5
1	Temperature of the absorber (position E)**	°C	5
1	Temperature of the cover	°C	2
1	Temperature of the surfaces of the room	°C	14
1	Room temperature	°C	3
1	Heat flow through the internal surface of the mass wall	W/m^2	-
2	Temperature of the mass wall (position A)**	°C	4
2	Temperature of the mass wall (position B)**	°C	4
2	Temperature of the mass wall (position C)**	°C	4
2	Temperature of the mass wall (position D)**	°C	4
2	Temperature of the internal side of the insulation panel	°C	2
2	Temperature of the external side of the insulating panel	°C	2
2	Air temperature at the top air gap	°C	1
2	Air temperature at the bottom air gap	°C	1
2	Temperature of the absorber	°C	2
2	Temperature of the cover	°C	4
2	Temperature of the surfaces of the room	°C	14
2	Room temperature	°C	3
2	Heat flow through the internal surface of the mass wall	W/m^2	-
Service room	Room temperature	°C	1
Climate	Total radiation on vertical south	W/m^2	-
Climate	Diffuse radiation on vertical south	W/m^2	-
Climate	Ambient temperature	°C	1
Climate	Wind speed along the south facade of the building	m/s	-

Table 2.2 The measuring points of the experiment with the two solar walls.
* number of junctions of the thermopiles, ** see fig. 2.21.
Wall 1 is the solar wall with the blind.
Wall 2 is the internally ventilated Trombe wall.

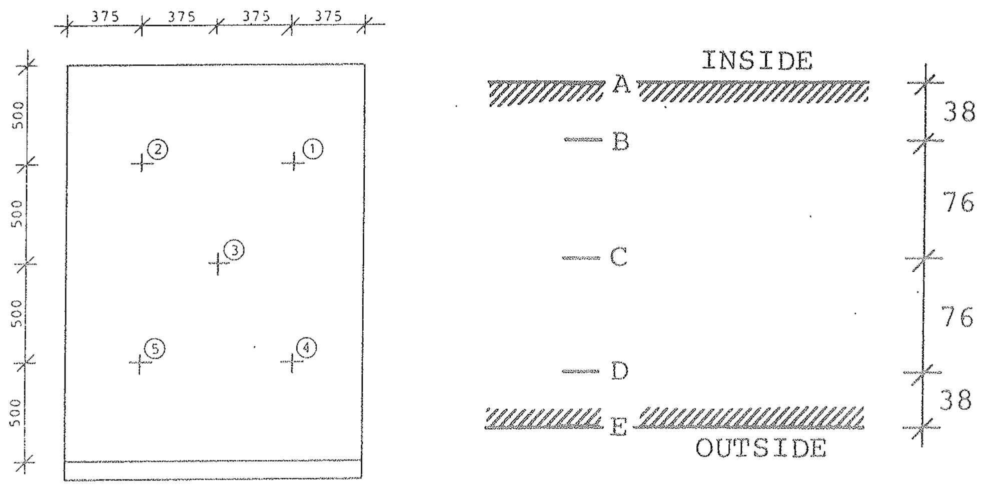

Figure 2.21 The location of the temperature measuring points of the mass walls. For wall 2 the middle thermocouples - location 3 - were disconnected.

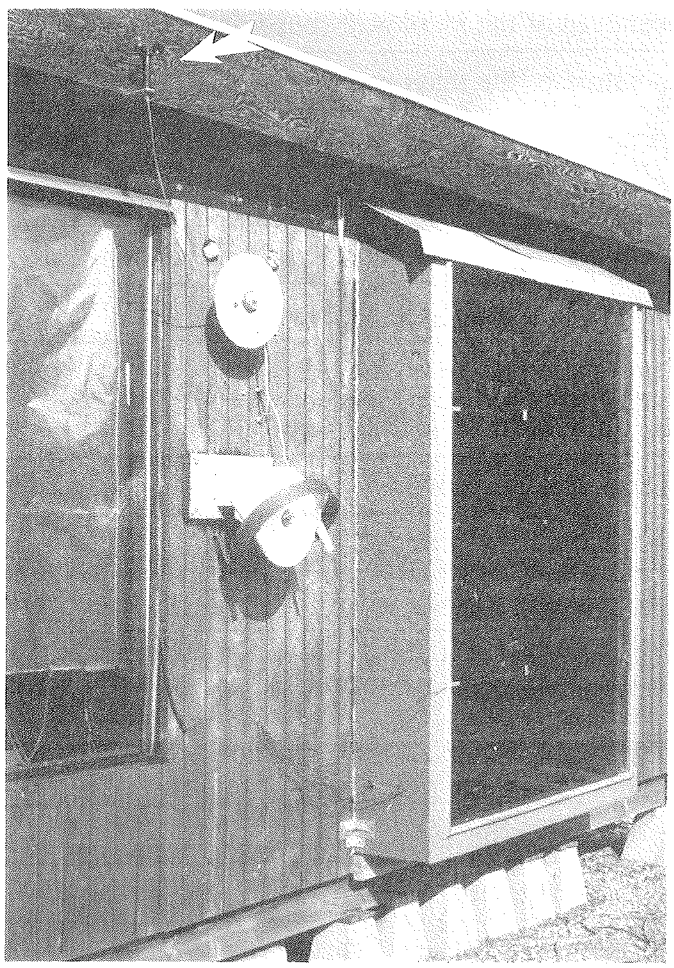

Figure 2.22 The pyranometers for measuring the total and diffuse radiation at vertical south. The cup anemometer for measuring the wind speed along the south facade was mounted on the verge board of the south facade - at the arrow.

3 Results from the experiment

The experiment with the two solar walls was carried out in the period January 30 to May 7, 1986. In the data set there are, however, three gaps: February 12, 4 am to February 17, 11 am, February 23, 24 pm to February 27, 1 am and April 3, 23 pm to April 21, 10 am.

The weather condition during the experiment is shown in fig. 3.1-3. Figure 3.1 shows the ambient temperature, fig. 3.2 shows the total and diffuse radiation on the south facade of the experimental building and fig. 3.3 shows the wind speed along the south facade of the experimental building. The data in the figures and in the following investigations are all averaged from 10 minute values to hourly values around each full hour. The value at eg 1:00 contains the average of the 10 minutely data from 0:30 to 1:30.

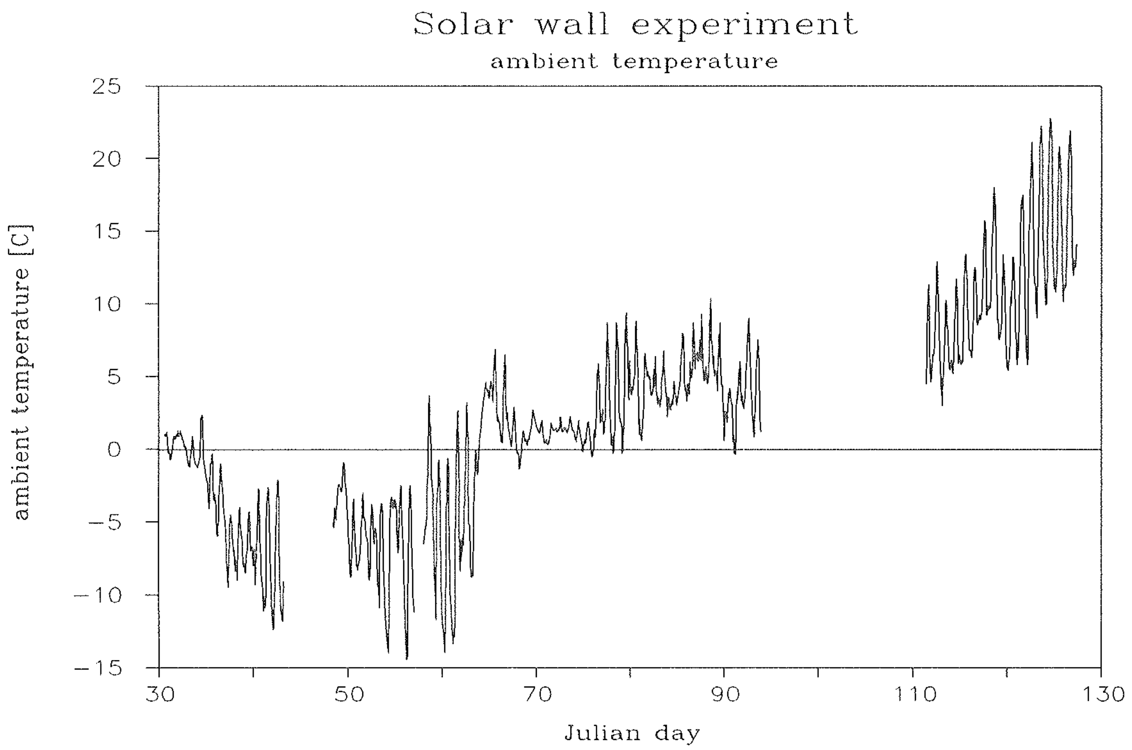

Figure 3.1 The ambient temperature during the experiment - January 30-May 7.

There were, as seen in fig. 3.2, problems with the pyranometers, used for measuring the solar radiation, during the first period. During the last period only the total radiation is shown as the measured diffuse radiation often turned out to be larger than the total radiation after the correction for the shading ring - see fig. 2.22. The reason for this is most probably that the shading ring was not properly adjusted so that the pyranometer was often measuring the total radiation.

Figure 3.4 shows the room temperature of room A and B (see fig. 2.1) with the solar walls. Figure 3.4 shows that the room temperatures were very unstable until day 60. Figure 3.5 shows the heat fluxes through the inner surfaces of the mass components - positive values are heat gains to the room, while negative values are heat losses. This figure illustrates also the unstable conditions until day 60. Especially the large heat loss from room B to the mass

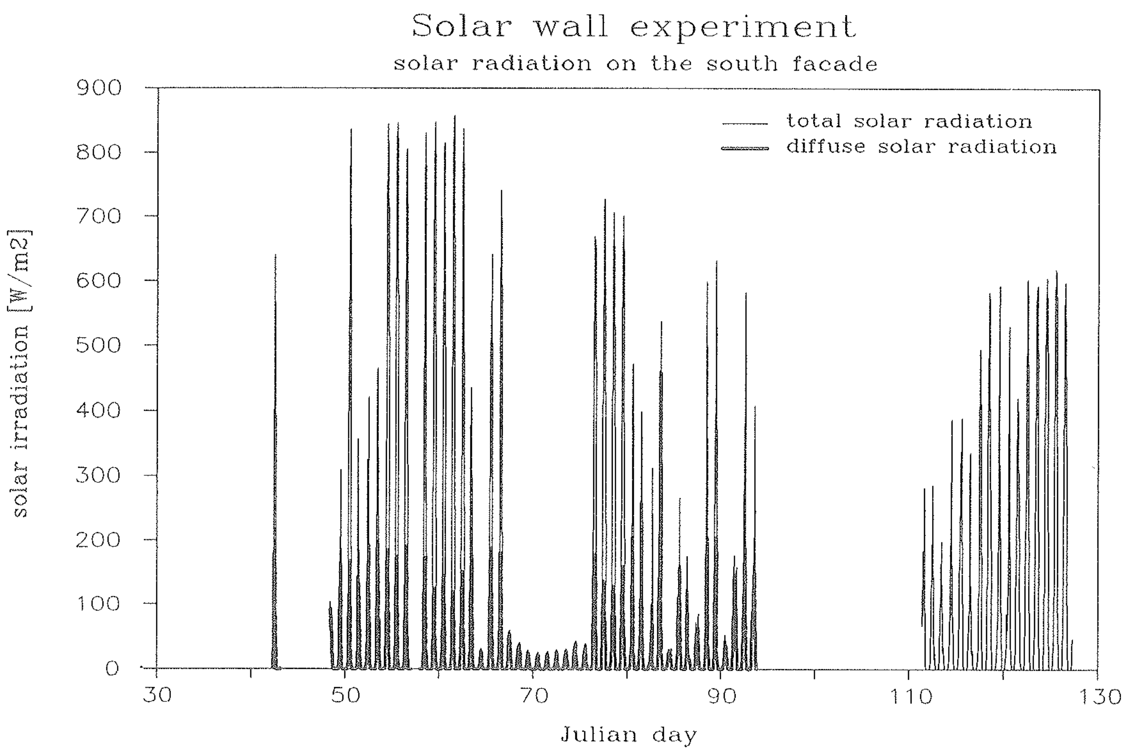

Figure 3.2 The total and diffuse solar irradiation on the south facade of the experimental building - January 30-May 7.

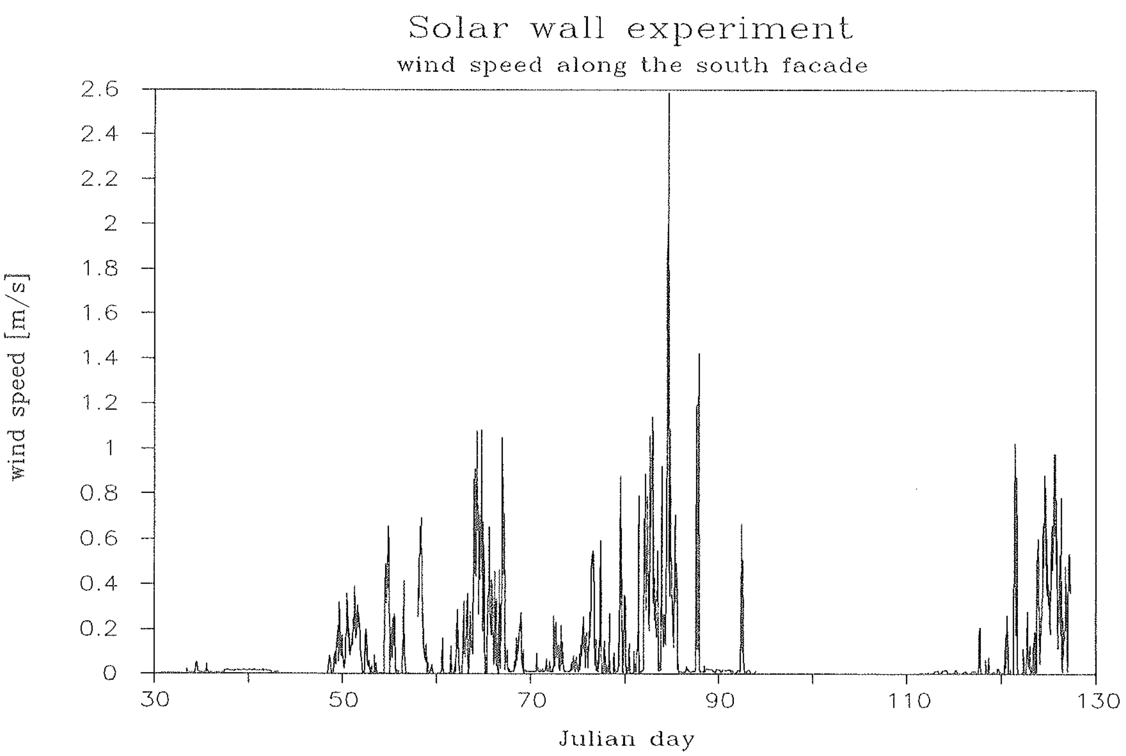

Figure 3.3 The wind speed along the south facade of the experimental building - January 30-May 7.

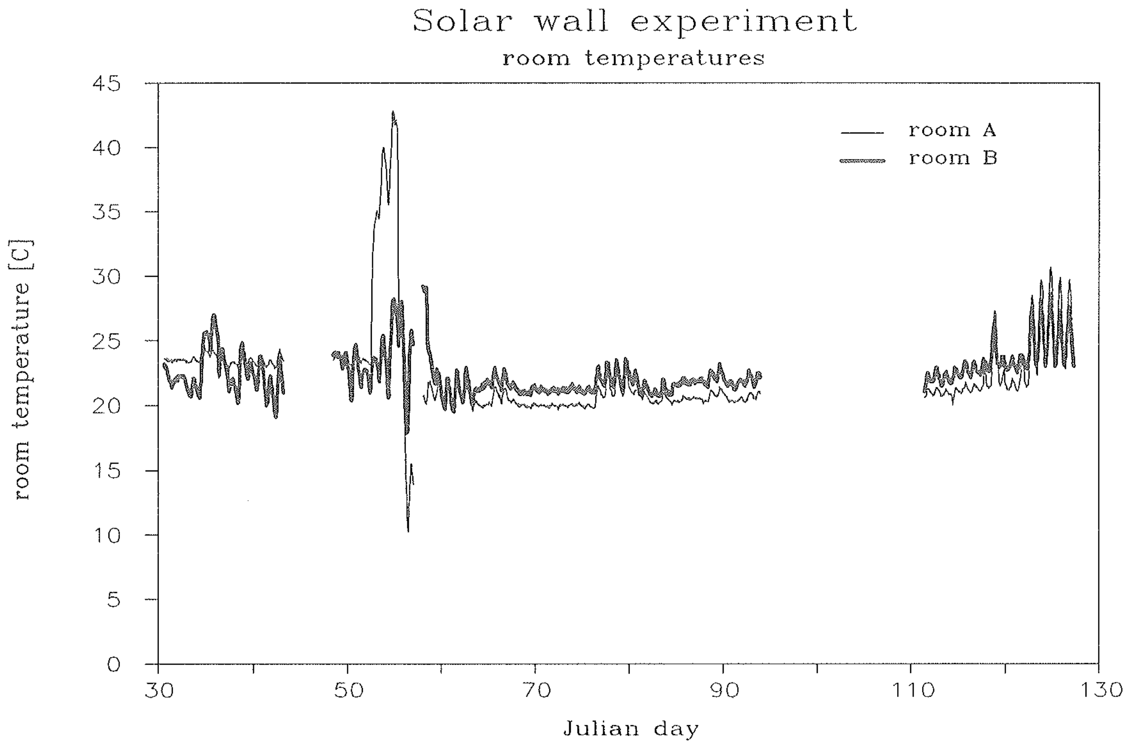

Figure 3.4 The air temperature of the test rooms during the experiment - January 30-May 7.

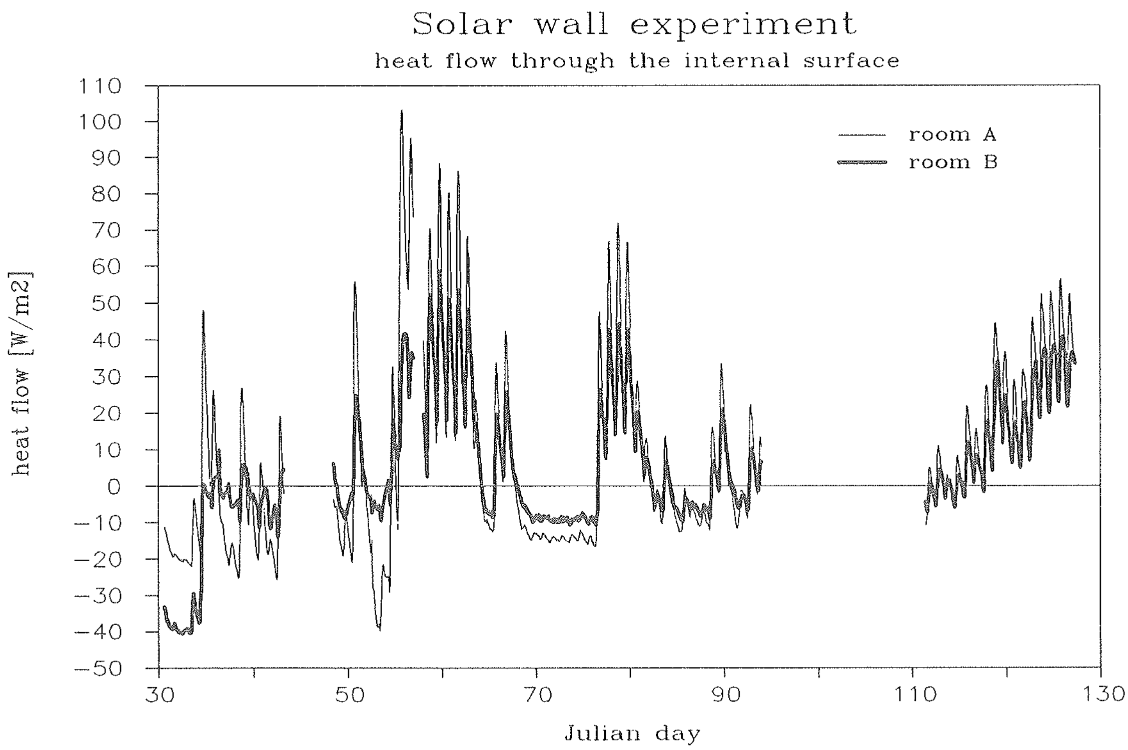

Figure 3.5 The heat fluxes through the internal surfaces of the mass components during the experiment - January 30-May 7.

component at the beginning of the experiment. The explanation for this may be, that the rooms were unheated until the beginning of the experiment. So the large "heat loss" was really heat input used to raise the temperature of the mass components to stable conditions.

Further investigations of the data set will, therefore, be limited to an investigation of the two periods March 1-April 3 and April 22-May 7.

3.1 Temperatures in the solar walls

In the following the temperatures measured in the solar walls during the experiment will be investigated.

The labels of the temperatures shown in the following graphs are given in fig. 3.6.

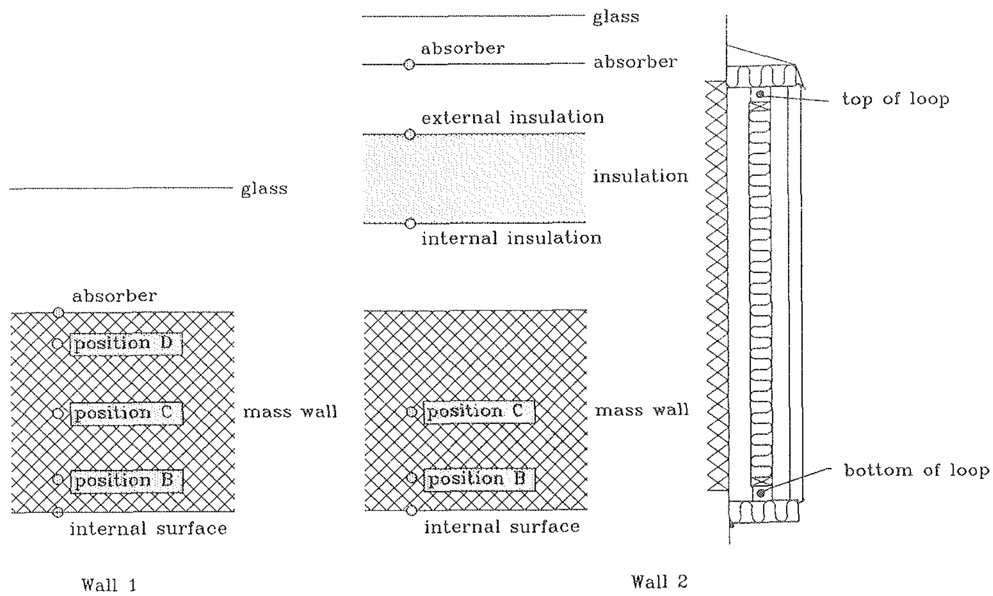

Figure 3.6 The labels of the temperatures shown in the following graphs.

No measurements were obtained for position D of the mass components of wall 2 due to a breakdown of the thermopile.

Figures 3.7-16 show the solar radiation and the temperatures of the walls for the first of the two investigated periods - March 1-April 3.

Wall 1 is the solar wall with the vertical turnable blind,
Wall 2 is the internally ventilated Trombe wall.

Please note that for wall 2 it is necessary to show the temperatures in two graphs.

Figures 3.8-10 can be rather difficult to interpret. Figure 3.11-16 show, therefore, the first and second week of the period in a close-up. The first week was a week with much solar radiation while during the second week, it was overcast.

Figures 3.17-20 show the solar radiation and the temperatures of the walls for the second of the two investigated periods - April 22-May 7.

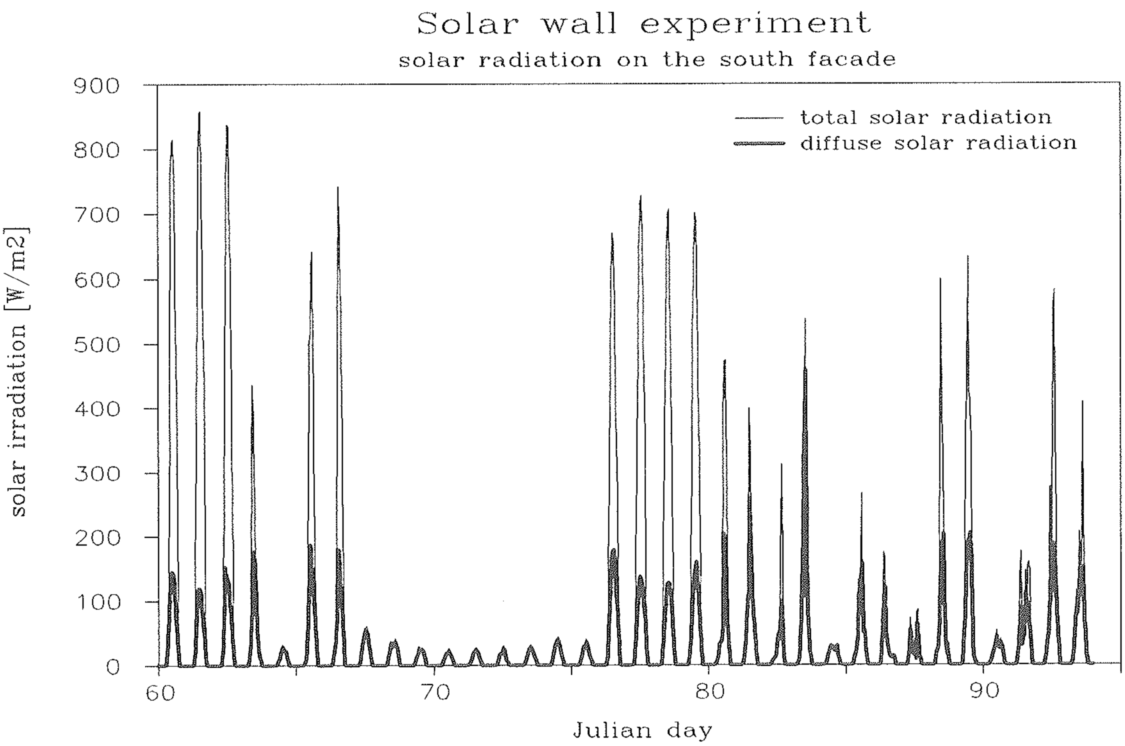

Figure 3.7 The total and diffuse solar irradiation on the south facade of the experimental building during the period March 1-April 3.

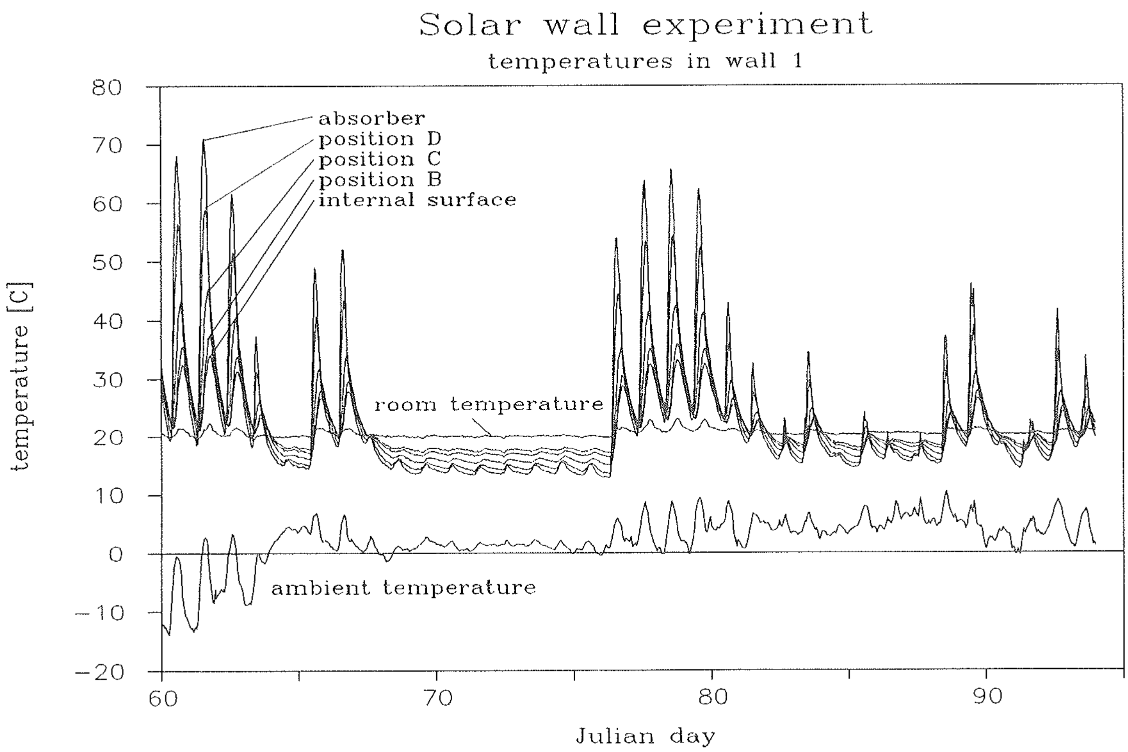

Figure 3.8 Temperatures in wall 1 during the period March 1-April 3.

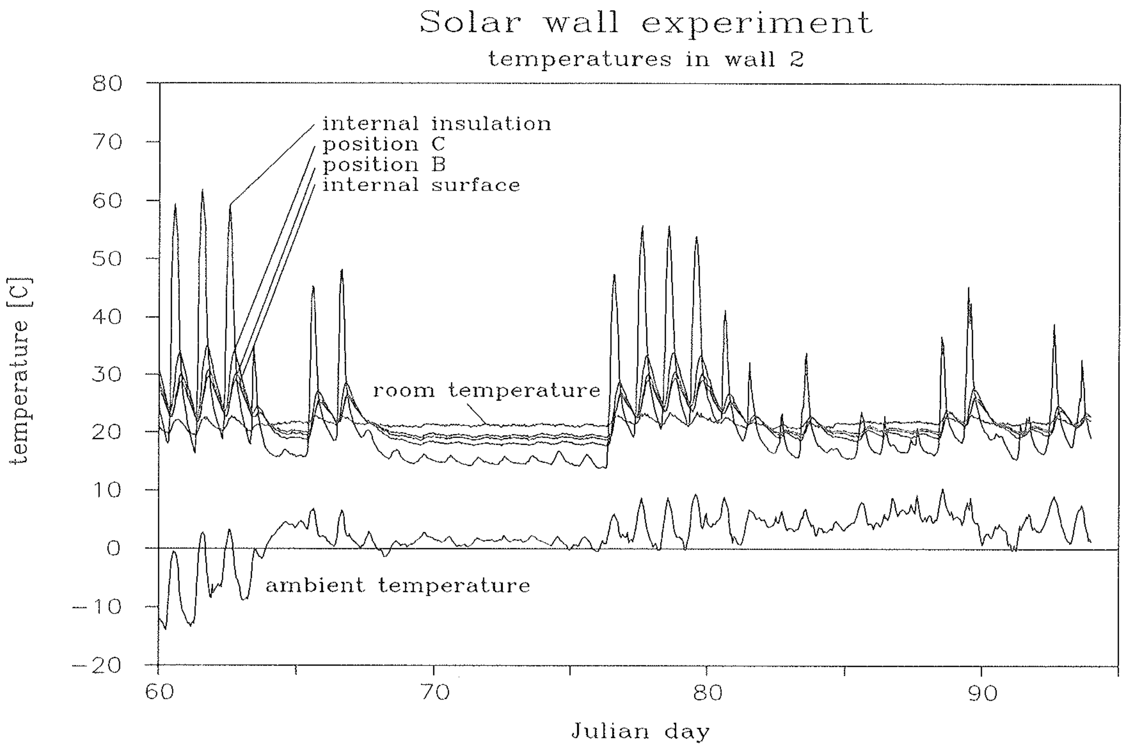

Figure 3.9 Temperatures in wall 2 during the period March 1-April 3.

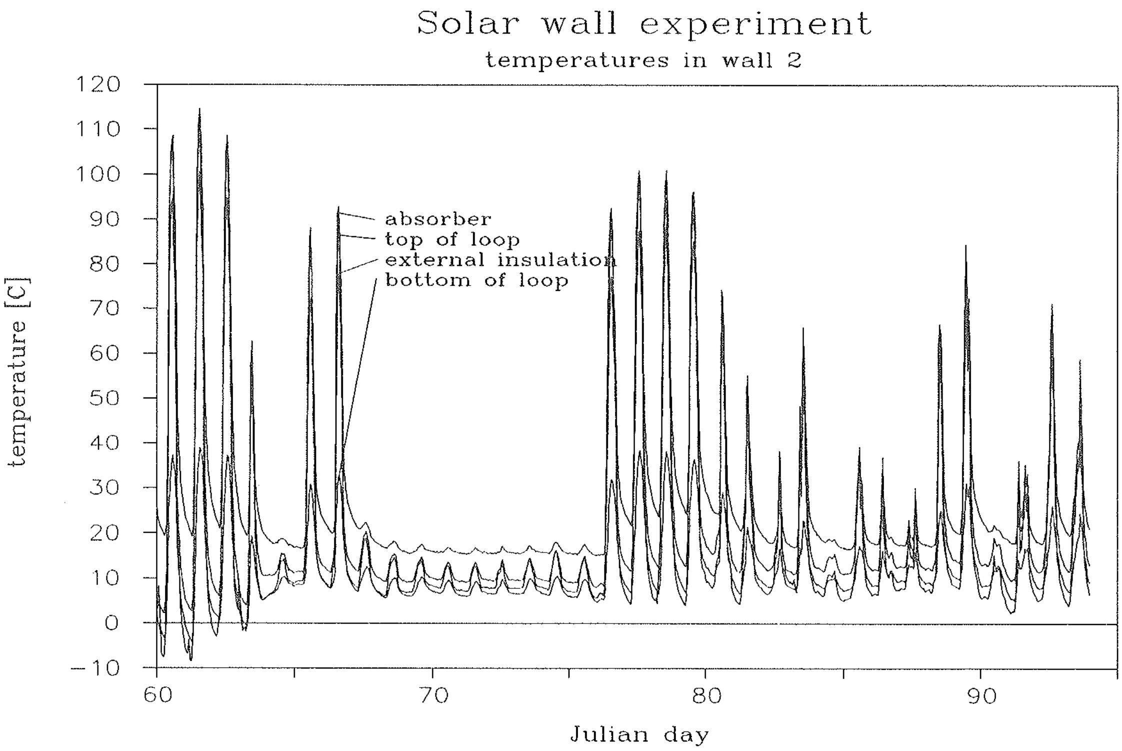

Figure 3.10 Temperatures in wall 2 during the period March 1-April 3.

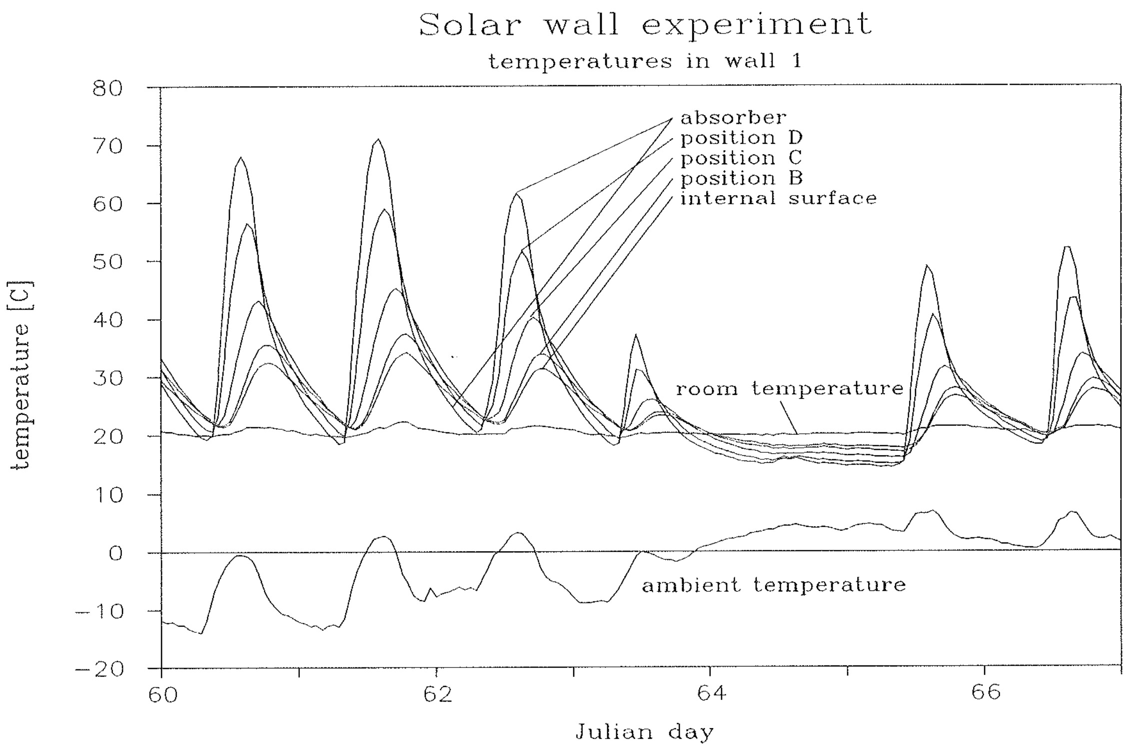

Figure 3.11 Temperatures in wall 1 during the period March 1-7 - a sunny period.

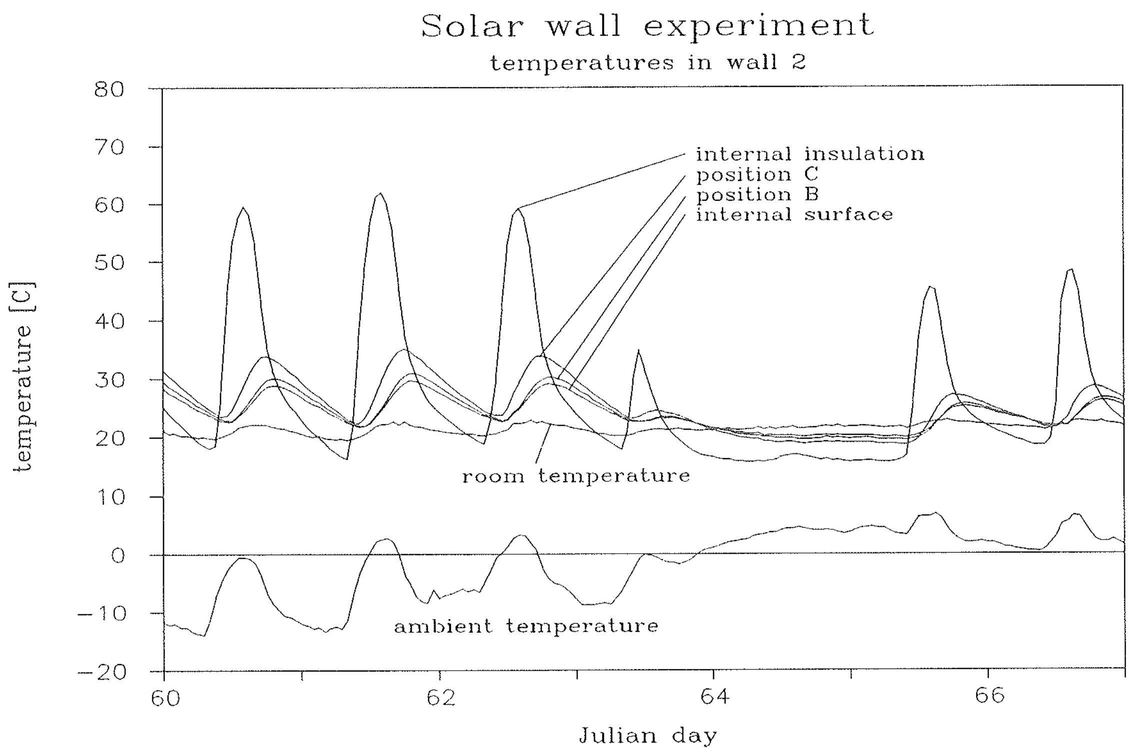

Figure 3.12 Temperatures in wall 2 during the period March 1-7 - a sunny period.

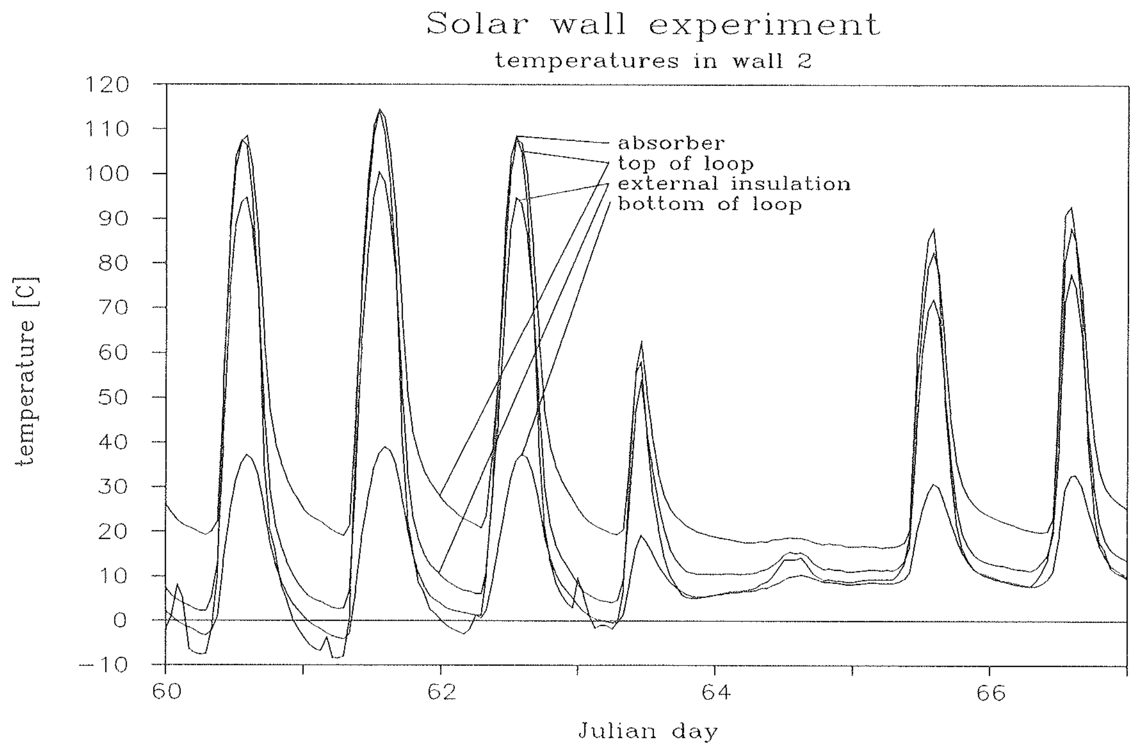

Figure 3.13 Temperatures in wall 2 during the period March 1-7 - a sunny period.

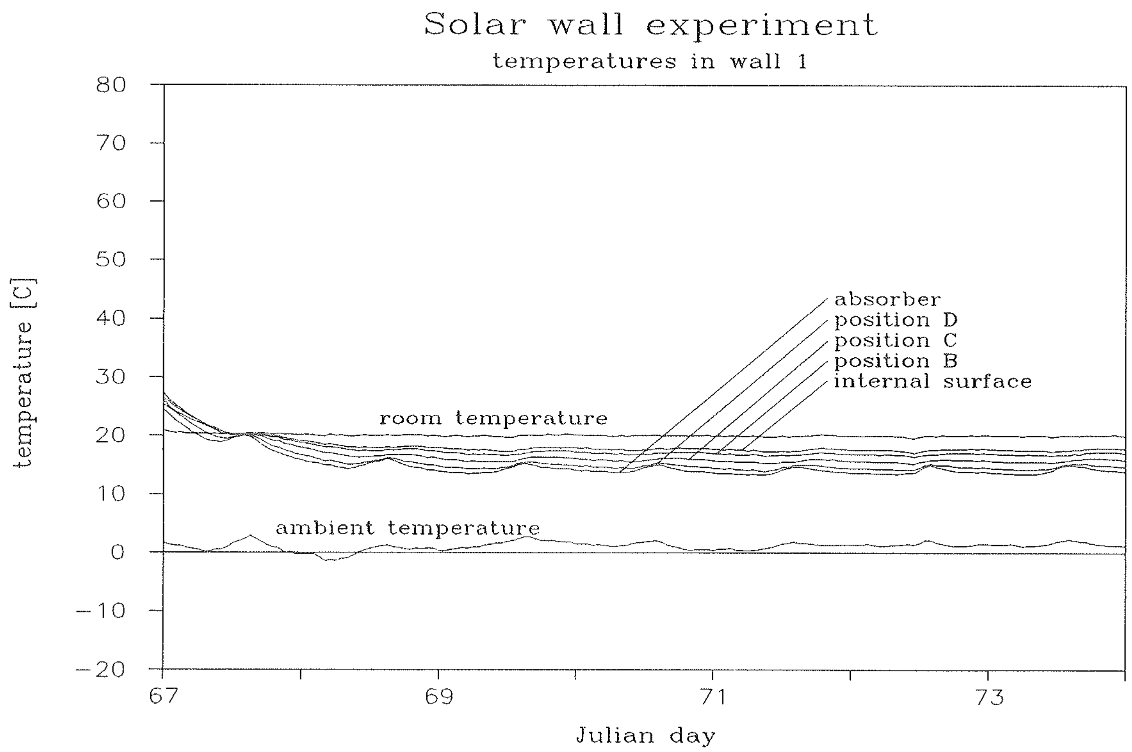

Figure 3.14 Temperatures in wall 1 during the period March 8-14 - an overcast period.

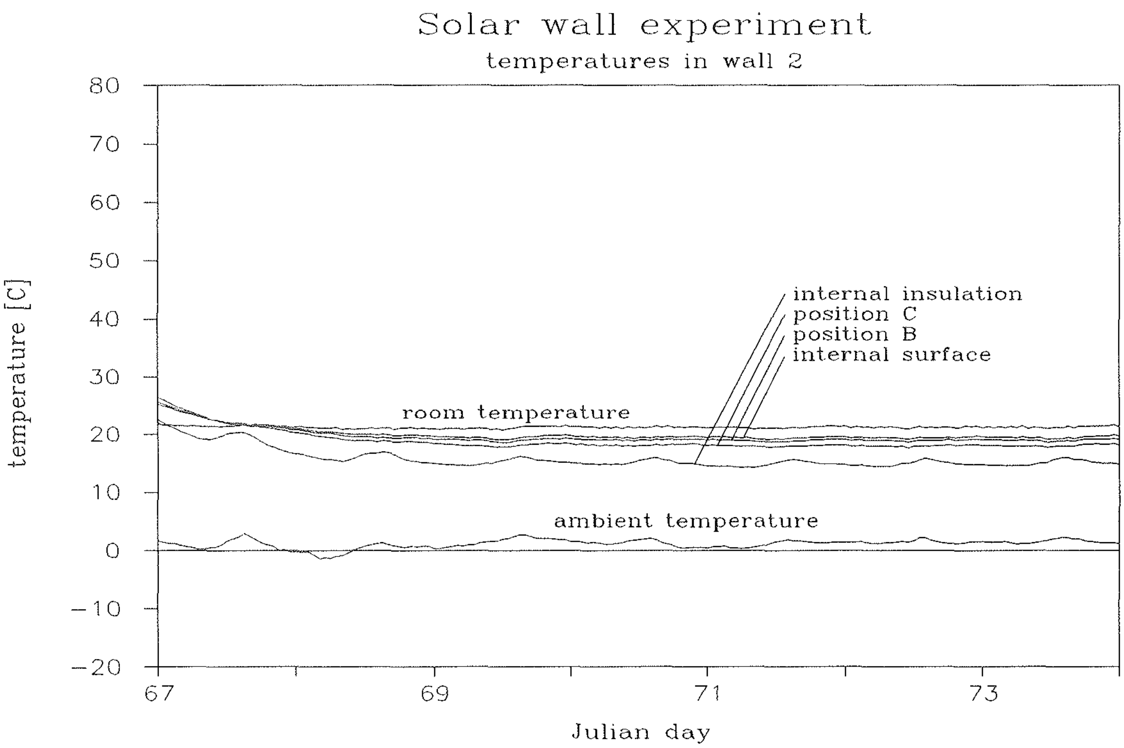

Figure 3.15 Temperatures in wall 2 during the period March 8-14 - an overcast period.

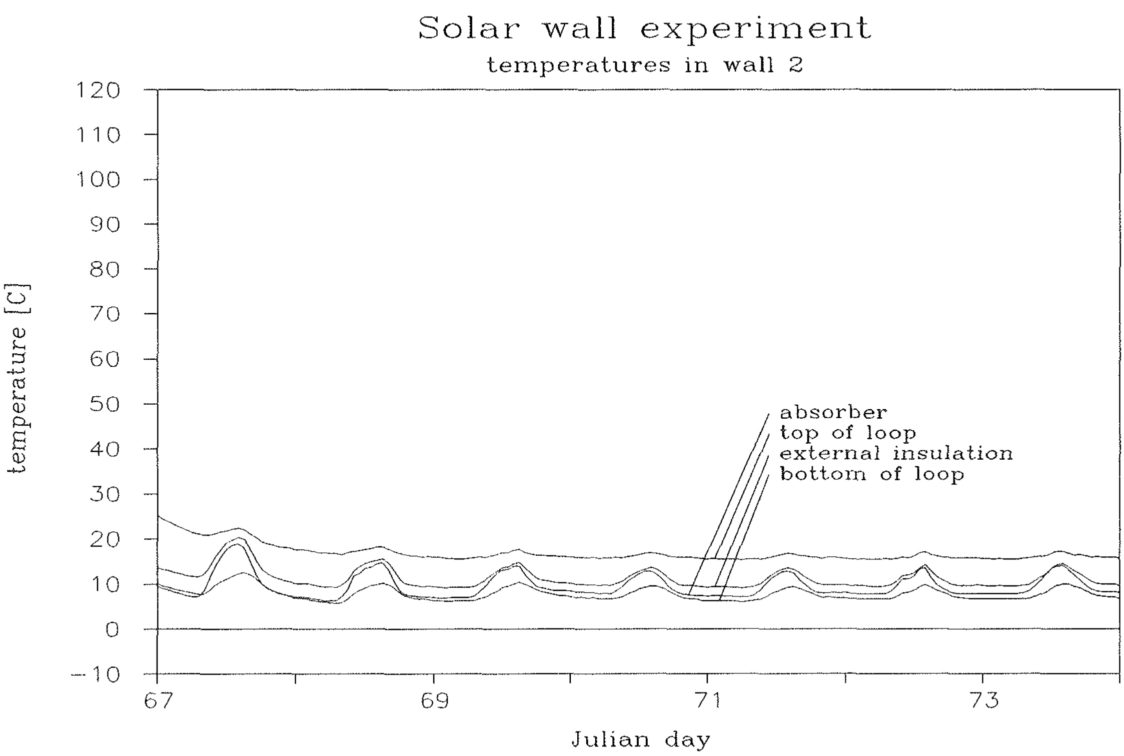

Figure 3.16 Temperatures in wall 2 during the period March 8-14 - an overcast period.

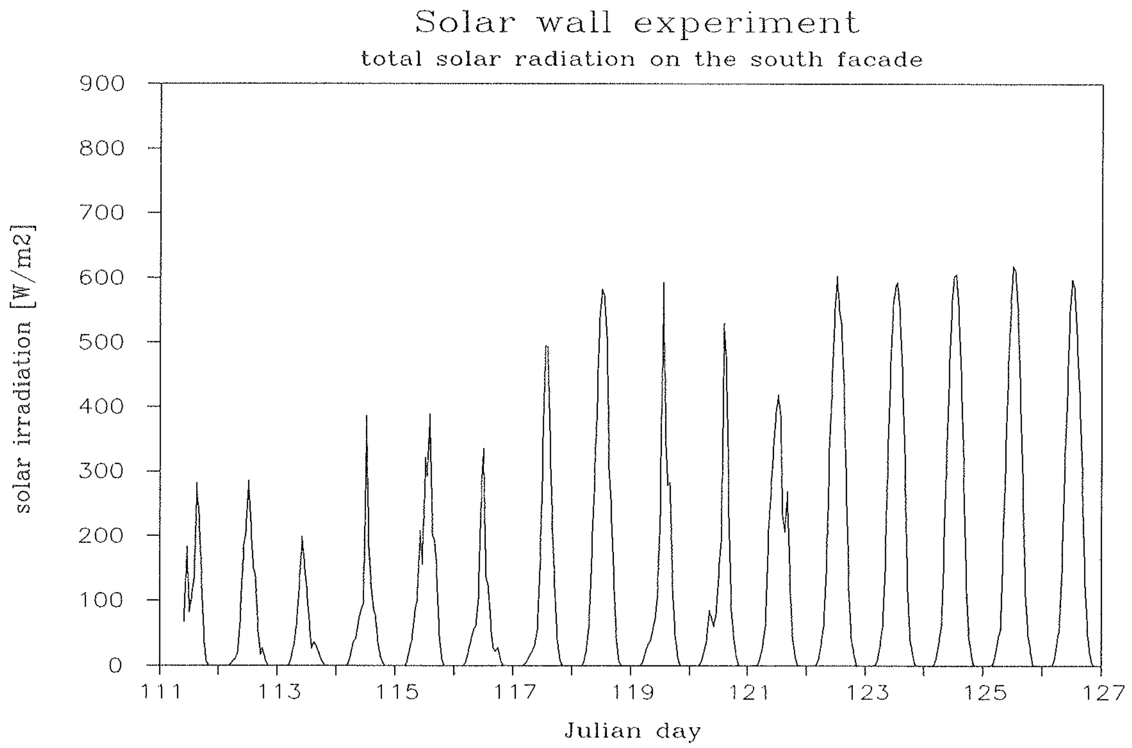

Figure 3.17 The total solar irradiation on the south facade of the experimental building during the period April 22-May 7.

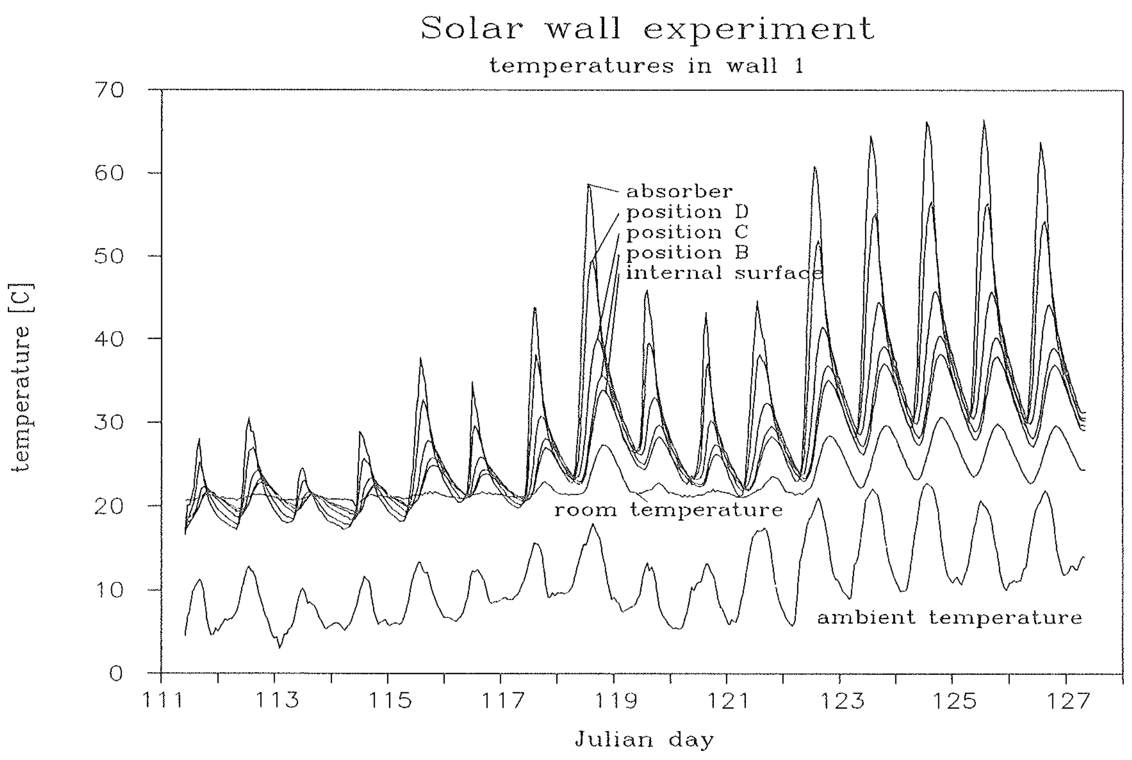

Figure 3.18 Temperatures in wall 1 during the period April 22-May 7.

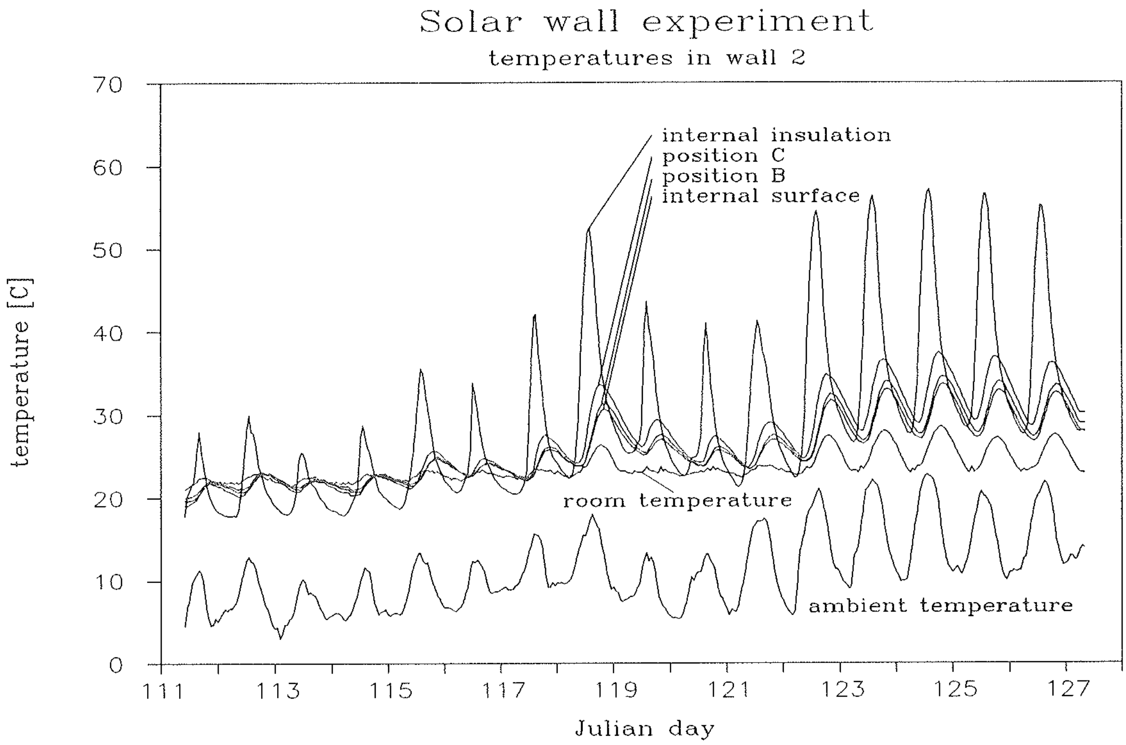

Figure 3.19 Temperatures in wall 2 during the period April 22-May 7.

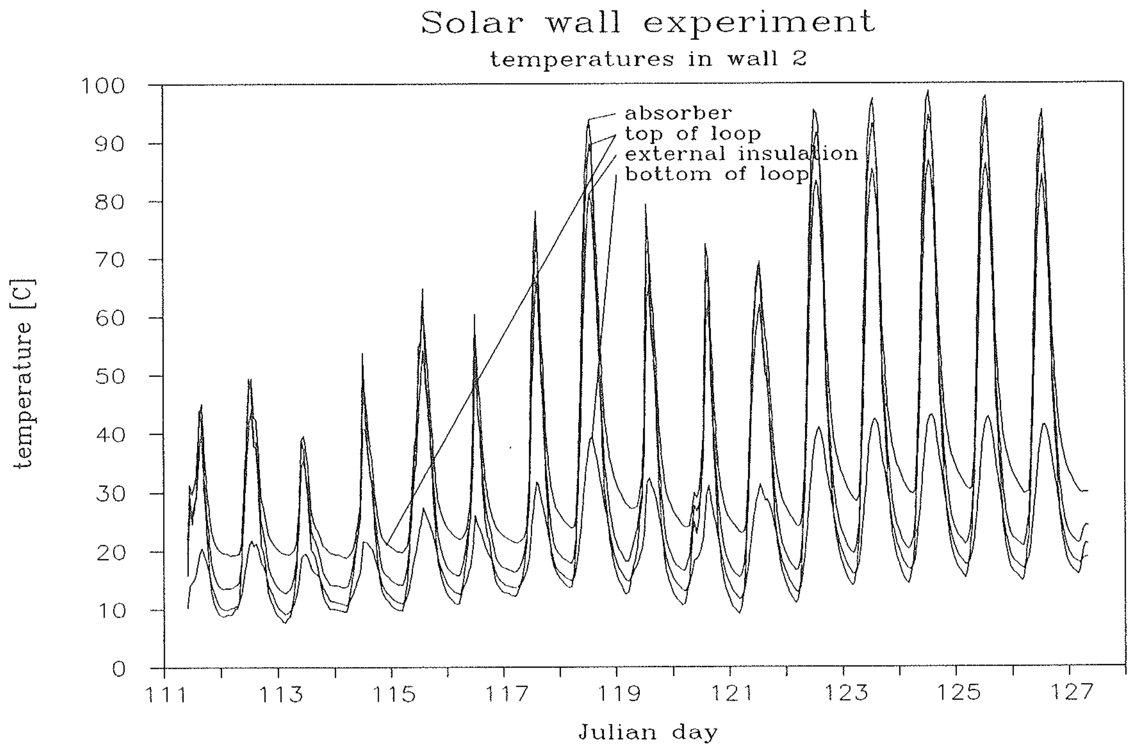

Figure 3.20 Temperatures in wall 2 during the period April 22-May 7.

An analysis of the figures shown on the previous pages reveals that during periods with solar radiation the absorber temperature is much higher for wall 2 (internally ventilated Trombe wall) than for wall 1 (with vertical turnable blind) se fig. 3.11 and 3.13 + fig. 3.18 and 3.20. This is, however, not surprising as the absorber in wall 1 was connected directly to the storage (the mass component) while for wall 2 the heat was transferred to the mass component by means of several heat transfer processes - from the absorber to the air of the outer air gap, from the outer to the inner air gap by means of a thermosiphon loop and from the air of the inner air gap to the mass component. The heat transfer from the absorber to the mass component is thus much slower in wall 2 than in wall 1.

Figs. 3.11-12 and 3.18-19 also show that the temperature level of the mass component in wall 1 is higher during periods with solar irradiation than that of the mass component in wall 2. The temperature level of the mass component in wall 1 decreases, however, more rapidly. This is because wall 1 was less insulated than wall 2. It is illustrated in fig. 3.11 and 3.13 where the temperature of the external surface of the insulation (with a position equivalent to the position of the absorber of wall 1) had a lower temperature during the night than the absorber of wall 1.

On the basis of the analysis of the graphs showing the measured temperatures of the solar walls during the experiment it may be concluded that wall 1 (with vertical turnable blind) has a higher solar gain than wall 2 (internally ventilated Trombe wall) but also a higher heat loss. This is also shown in fig. 3.5 where the heat flux through the surface of the mass components is shown. The air temperature level of the two rooms where, however, not equal as shown in fig 3.4, so an investigation on mean key values obtained from the experiment is necessary in order to determine which wall had the best performance.

3.2 Investigation of mean key values for the solar walls

In this section some mean key values for the solar walls - U-value, overall heat gain and solar gain - derived from the experiment will be investigated.

3.2.1 U-values

In order to calculate an apparent U-value of the walls based on the measurements there is a need for a period with stable conditions - a period without much solar irradiation. Fortunately such a period occurred during the experiment - day 69-75 (both days inclusive), where it was overcast and a rather stable ambient temperature resulting in rather stable heat fluxes through the mass components - see figs. 3.1-3 and 3.5.

In order to ensure, that the condition in the mass walls was stable, only the period 70-75 has been used for the calculation of the U-values. Table 3.1 shows the different input values for calculating the U-values and the apparent U-values for the two solar walls.

Wall	heat loss W/m2	ambient temperature °C	room temperature °C	U-value W/m2K
1	14.2	1.2	20.0	0.76
2	9.0	1.2	21.2	0.45

Table 3.1 The calculated apperent U-values of the solar walls based on the measurements.

In order to investigate if the U-values from table 3.1 are reasonable the theoretical U-values have been calculated. For wall 1 (with the blind) the U-value has been calculated both for open (actually no blind) and closed blind - this is shown in table 3.2. The theoretical U-value for wall 2 (internally ventilated Trombe wall) is, however, more difficult to calculate as the wall contains an inhomogeneous construction - the insulated panel. It is in the calculations taken into consideration that 13 % of the insulating panel (= 11.5 % of the transparent area) was made of wood while the rest was filled with mineral wool and that the area of the two dampers constituted 11 % of the transparent area. For such constructions the Danish standard [4] advices to calculated two U-values - U' and U''. For U' a new "mean" λ-value (λ') is calculated for the inhomogeneous layer, while for U'' the three parts of the wall (insulated part, wooden part and damper part) are regarded as separate transmission areas. U' is calculated in figure 3.21 and table 3.3 and U'' in table 3.4. The U-value is calculated as:

$$U = \frac{2U'U''}{U'+U''}$$

The influence of the thermo laths is not considered for any of the walls.

Material	thickness	λ-value	Open blind		Closed blind	
	mm	W/mK	resistance Km2/W	U-value W/m2K	resistance Km2/W	U-value W/m2K
sand/lime bricks	228	0.95	0.24		0.24	
air gap(s)	148 or 2 x 74		0.35		2 x 0.47	
glass	5	0.81	0.006		0.006	
thermal surface resistances			0.17		0.17	
Total			0.766	1.31	1.356	0.74

Table 3.2 The theoretical U-value of wall 1 with open and closed blind. The influence of the thermo laths has not been considered.

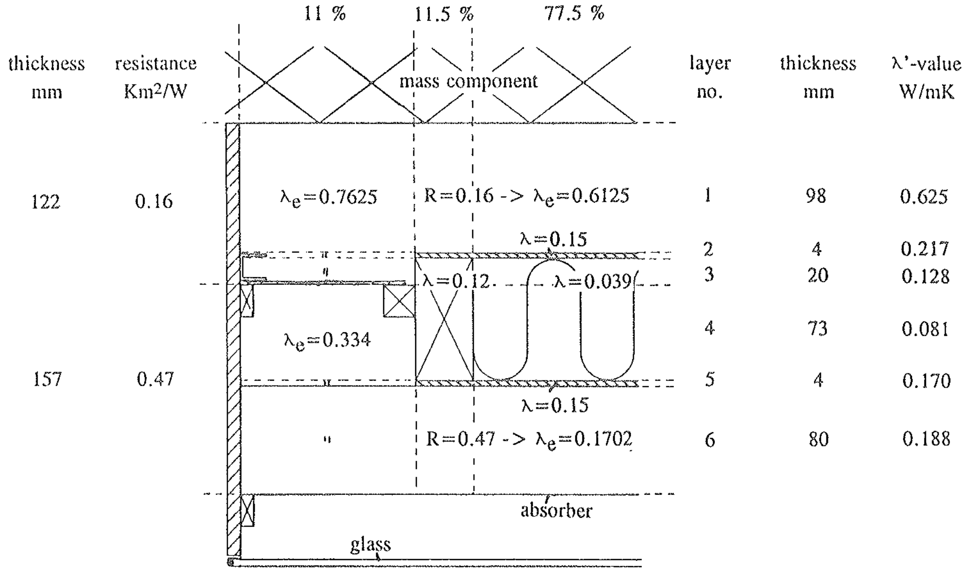

Figure 3.21 The figure shows how the λ'-values have been calculated for the inhomogeneous parts of wall 2. It was necessary to divide the air gap/insulated panel/air gap into 6 inhomogeneous layers. The λ'-value of layer 3 is eg calculated as 0.11*0.7625+0.115*0.12+0.775*0.039 = 0.128.

Material	thickness mm	λ-value W/mK	resistance Km²/W	U'-value W/m²K
sand/lime bricks	228	0.95	0.24	
layer 1*	98	0.625	0.157	
layer 2*	4	0.217	0.018	
layer 3*	20	0.128	0.156	
layer 4*	73	0.081	0.901	
layer 5*	4	0.170	0.024	
layer 6*	80	0.188	0.426	
air gap	55		0.35	
glass	5	0.81	0.006	
thermal surface resistances			0.17	
Total			2.448	0.41

Table 3.3 The U'-value of wall 2. The influence of the thermo laths has not been considered.
* thickness and λ'-value are from figure 3.21.

The U-value of wall 2 is thus 2*0.41*0.33/(0.41+0.33) = 0.37 W/m²K.

Material	thickness mm	λ-value W/mK	insulated part resistance Km^2/W	wooden part resistance Km^2/W	damper part resistance Km^2/W	U''-value W/m^2K
sand/lime bricks	228	0.95	0.24	0.24	0.24	
air gap	98		0.16	0.16	0.16	
masonite	4	0.15	0.027	0.027	0.027	
mineral wool	93	0.039	2.385	-	-	
wood	93	0.12	-	0.775	-	
masonite	4	0.15	0.027	0.027	0.027	
air gap	80		0.47	0.47	0.47	
aluminium	1	200	-	-	-	
air gap	55		0.35	0.35	0.35	
glass	5	0.81	0.006	0.006	0.006	
thermal surface resistances			0.17	0.17	0.17	
sum of resistances			3.835	2.225	1.45	
part of wall %			77.5	11.5	11	0.33

Table 3.4 The U''-value of wall 2. The influence of the thermo laths has not been considered.

When comparing the theoretical U-values with the U-values derived from the measurements (the actual U-values) it is seen that the actual U-value of wall 1 is better than expected. It is very close to the theoretical U-value for the wall with closed blind. The blind thus reduces the convective and radiative heat loss very much even when it is open.

The actual heat loss of wall 2 is only 22 % higher than the theoretical heat loss. The higher actual heat loss may be explained by the large uncertainties on the measurements and the calculations, but also by the fact that the influence of the heat loss through the thermo laths has not been considered for the theoretical U-value. It thus seems that the dampers of the insulated panel (plastic foil and a grid) did operate as expected during periods without solar radiation, so that the mass component was not discharged due to a reverse circulation of air between the two air gaps. On fig. 3.13 it is, however, seen that the temperature just outside the top damper is 10-15°C higher than the temperature on the external side of the insulating panel. This higher temperature is believed to be caused by the poor thermal resistance of the damper, which tends to create a warmer zone at the top of the air gap in front of the insulated panel during periods without solar radiation.

According to the Danish building regulations [5] the U-value of a traditional heavy wall facing the outside should be below 0.35 W/m²K. The U-value of wall 1 is twice as high as this value but still only half the value of a solar wall with only a single-pane cover in front of the mass component. The U-value of wall 2 is only about 30 % higher than that of a traditional wall.

3.2.2 Overall net heat gains

The overall net heat gain has been summarized for the two periods March 1-April 3 and April 22-May 7. This is shown in table 3.5. The walls gave in average almost no heat input to the rooms during the first period - it was in the same order of magnitude as the heat loss. The saved heat loss during this period was, however, large as seen later - table 3.7-8.

Period	Wall 1 Wh/m²	Wall 2 Wh/m²
March 1-April 3	51	44
April 22-May 7	7906	5701

Table 3.5 The measured net heat flux through the internal surface of the mass components = the heat gain.

However, table 3.5 is not giving a true picture of the performance of the walls as the air temperature of the rooms was not identical as shown in fig. 3.5. The mean values of the room temperatures for the two periods are shown in table 3.6 together with the ambient temperature.

Period	Room A °C	Room B °C	Ambient temperature °C
March 1-April 3	20.5	21.4	2.3
April 22-May 7	23.1	23.6	11.3

Table 3.6 The average air temperature of the rooms and the ambient temperature during the two periods.

The temperature of room B with wall 2 was most of the time higher than room A with wall 1. The heat loss through wall 2 was thus too high and the solar gain too low for performing a fair comparison between the walls.

The performance of wall 2, judged by the overall net heat gain, was 14 % lower than the performance of wall 1 for the first period and 28 % lower for the second period. Although the temperature level of room B was somewhat higher than room A, it cannot account for the difference. It may thus be concluded, that the performance of wall 1 was higher than that of wall 2 for the given period. The periods had, however, a lot of solar radiation. If the experiment had run for the whole heating season the conclusion may have been different as the solar radiation in Denmark during the period November-January is normally very low. The higher U-value of wall 1 would decrease the performance of this wall compared to wall 2.

The only way to determine which wall is best, is to develop models of the walls and simulate the annual heat savings with both walls installed in buildings. It was, however, not the aim of the project to create models of the walls. It would further be difficult to develop reliable models of the walls. The models of the walls should be validated by comparing the performance of the models of the walls with the measurements. No thermo-physical properties of the materials of the walls have, however, been measured, the thermal bridges introduced by the thermo laths are difficult to describe and the mass components are suspected to have contained some water so the heat transport through them may not only be due to conduction. Agreement between measurements and predictions can, therefore, always be obtained by fitting the input data to the model. So there is no idea in performing such a validation study using the measured data from this experiment. Wall 1 is furthermore very difficult to model as the thermo-physical and optical properties of the gap between the mass component and the cover change over the day because of the operation of the blind.

It is, however, anticipated that the solar walls will cover a part of the heat demand of the building. More detailed analyses are, however, necessary in order to determine if the walls are profitable.

3.2.3 Solar gains

The solar gain is the overall gain plus the heat loss. The solar gain has been calculated by using the overall gains from table 3.5 and calculating the heat losses using the U-values from table 3.1 and the temperatures from table 3.6. This is shown in tables 3.7-8.

Period	Overall gain Wh/m^2	Heat loss Wh/m^2	Solar gain Wh/m^2
March 1-April 3	51	11287	11338
April 22-May 7	7906	3435	11341

Table 3.7 The solar gains from wall 1.

Period	Overall gain Wh/m²	Heat loss Wh/m²	Solar gain Wh/m²
March 1-April 3	44	7014	7058
April 22-May 7	5701	2120	7821

Table 3.8 The solar gains from wall 2.

The total solar radiation on the walls was during the two periods 62.306 and 43.546 Wh/m² respectively. Table 3.9-10 shows the efficiency of the two wall for the two periods

Period	Solar gain Wh/m²	Total solar radiation Wh/m²	Efficiency %
March 1-April 3	11338	62306	18
April 22-May 7	11341	43546	26

Table 3.9 The efficiency of wall 1.

Period	Solar gain Wh/m²	Total solar radiation Wh/m²	Efficiency %
March 1-April 3	7058	62306	11
April 22-May 7	7821	43546	18

Table 3.10 The efficiency of wall 2.

Tables 3.7-10 show what has already been mentioned, that the solar gain for wall 1 was larger than that of wall 2. Wall 1 loses, however, much of the gained energy, compared to wall 2, due to a larger heat loss. Table 3.9-10 shows further that the increase in the efficiency of the walls from period 1 to period 2 is higher for wall 2 than for wall 1.

3.2.4 Thermal comfort

The internal surface temperature of the mass component fluctuates very much as seen in figs. 3.11-12 and 3.18-19. This may cause problems for the thermal comfort in the rooms as surface temperatures very different from the room temperature may result in discomfort.

Figures 3.22-25 show the internal surface temperature of the mass components for the two periods. The surface temperatures are compared to the air temperature of the rooms and the mean temperature of the other surfaces of the rooms.

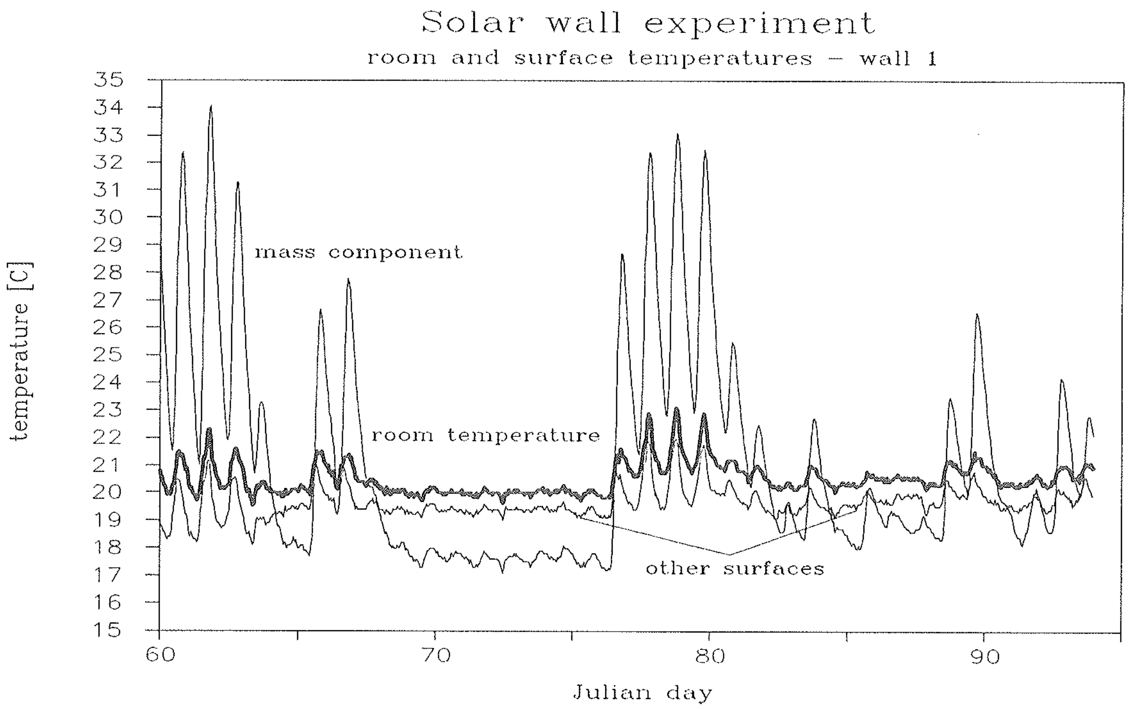

Figure 3.22 The internal surface temperature of the mass component of wall 1 for the first period compared to the air temperature of the room and the mean temperature of the other surfaces.

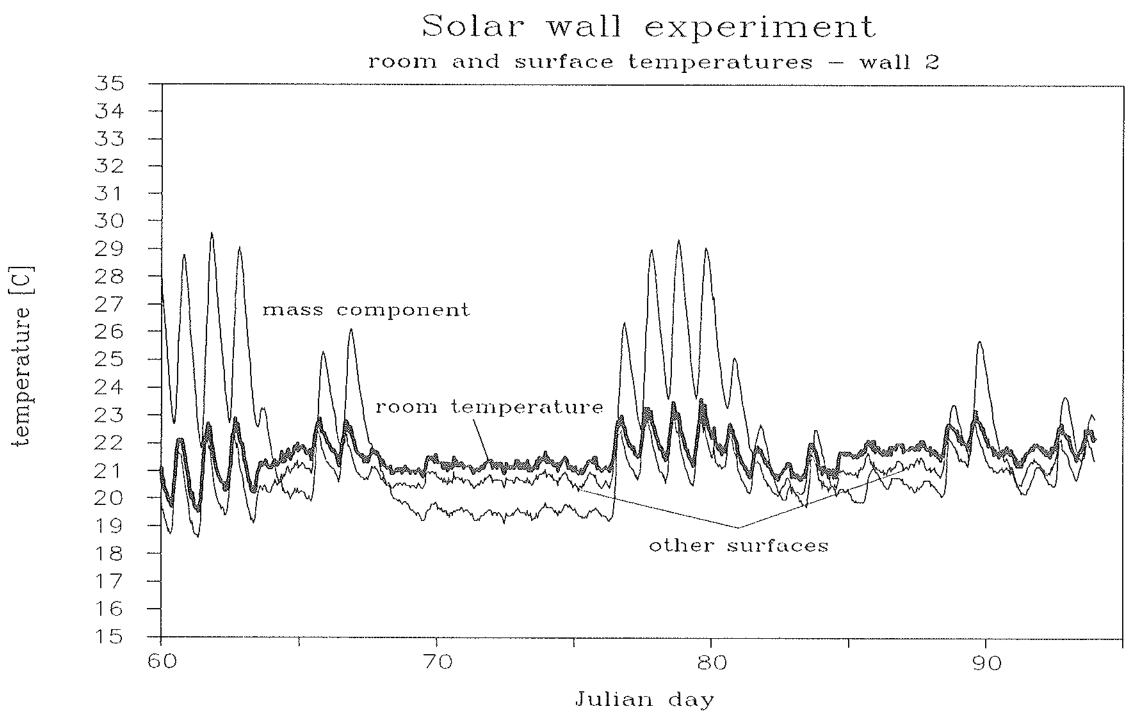

Figure 3.23 The internal surface temperature of the mass component of wall 2 for the first period compared to the air temperature of the room and the mean temperature of the other surfaces.

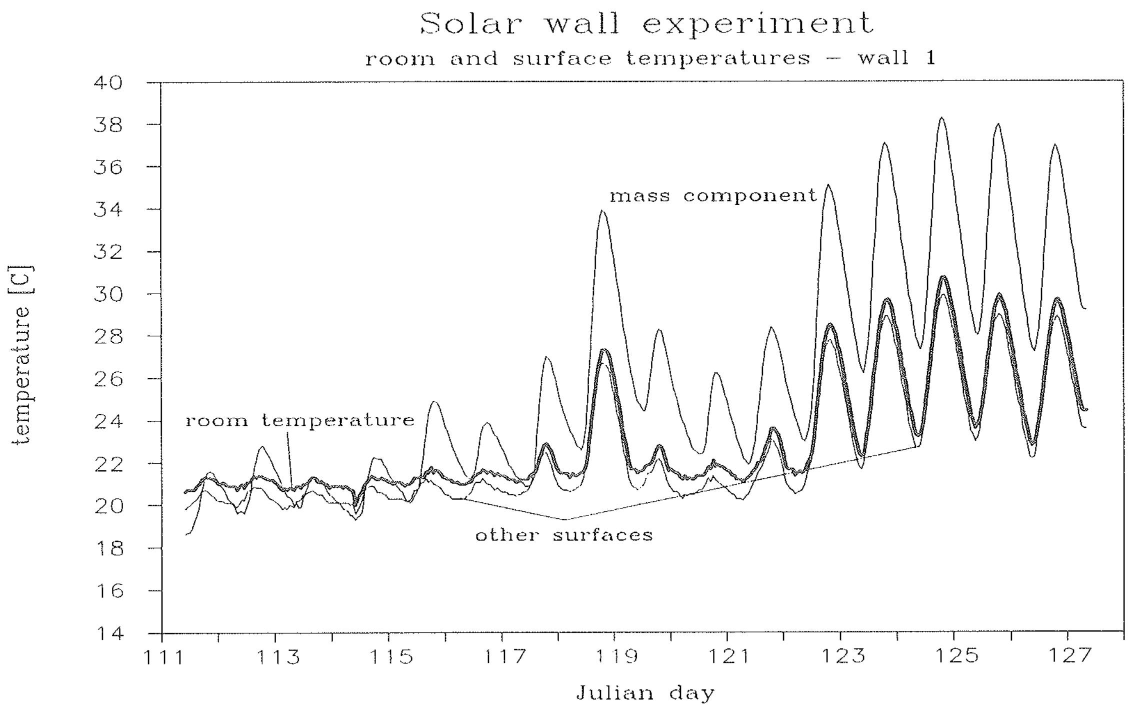

Figure 3.24 The internal surface temperature of the mass component of wall 1 for the second period compared to the air temperature of the room and the mean temperature of the other surfaces.

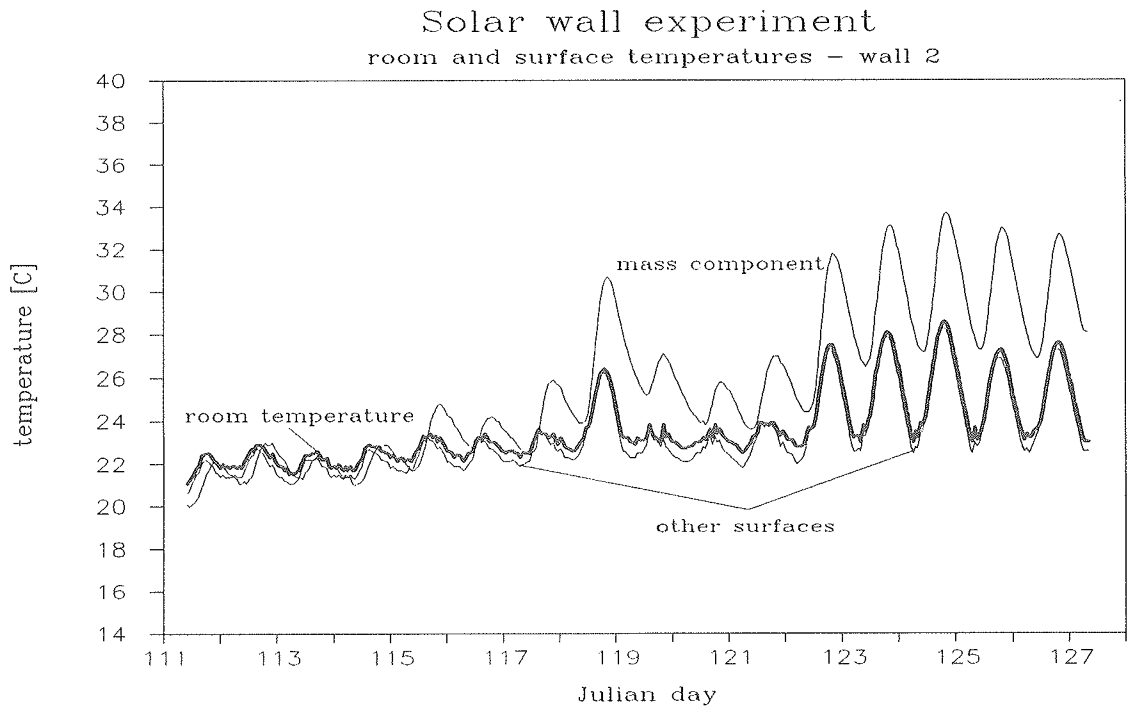

Figure 3.25 The internal surface temperature of the mass component of wall 2 for the second period compared to the air temperature of the room and the mean temperature of the other surfaces.

The figures show that discomfort will mainly occur in connection with wall 1, as the surface temperature of this wall fluctuates more than the surface temperature of wall 2. This was also expected as this wall has the highest solar gain resulting in high temperatures of the wall and the highest U-value resulting in low temperature of the wall.

Figures 3.24-25 further show that serious overheating problems may occur for both walls during summer periods. However, this does not need to be the case as the walls have a built-in overheating protection. If the mechanism for turning the slats of the blind is switched off in a position where the blind is closed, then much of the incoming solar radiation will be reflected out again and thus heat up the wall less.

A way to reduce the heat loss of wall 1 is to install transparent insulation on the absorber. This will, however, increase the overheating problems during summer periods, but again the blind will prevent this if operated correctly.

If one or two additional simple manually driven dampers were installed in the top and/or bottom air gap of wall 2, it would be possible, during summer periods, to convert the wall to a more or less normal wall ie the heat will no longer be transferred by an air stream but has to be transported through the insulated panel by conduction. This will decrease the overheating problems considerably.

This is illustrated in fig. 3.26. Figure 3.26 shows the temperatures in the two air gaps of a ventilated Trombe wall together with the room and ambient temperatures, the global radiation on the cover of the Trombe wall and an indication of when the top damper was closed or open. The Trombe wall was tested in the Danish PASSYS test cell under the CEC concerted action PASSYS (ref. [6]). The Trombe wall was somewhat different from the wall shown in fig. 1.1. The principle of the wall is shown in fig. 3.27 - further details may be found in ref. [7]. There was no separate absorber in the wall. The absorber was mounted on the insulating panel. The two plastic foil dampers were replaced by only one motor driven damper at the top of the insulating panel.

The experiment shown in fig. 3.26 was performed during a period with much solar radiation and relatively high ambient temperature. The heavily insulated test cell was free floating ie no cooling to reduce the room temperature of the test room behind the Trombe wall.

From fig. 3.26 it is seen that the temperature level of the mass component may decrease considerably if it is made possible to close the dampers of an internally ventilated Trombe wall during summer-time. The decrease of the temperature level will in actual walls be lower than shown in fig. 3.26 as the room temperature in normal buildings will be maintained at a temperature level below 25°C. The duration of the period with closed damper in fig. 3.26 was further too short for allowing the temperature of the mass wall to be lowered to a stable level.

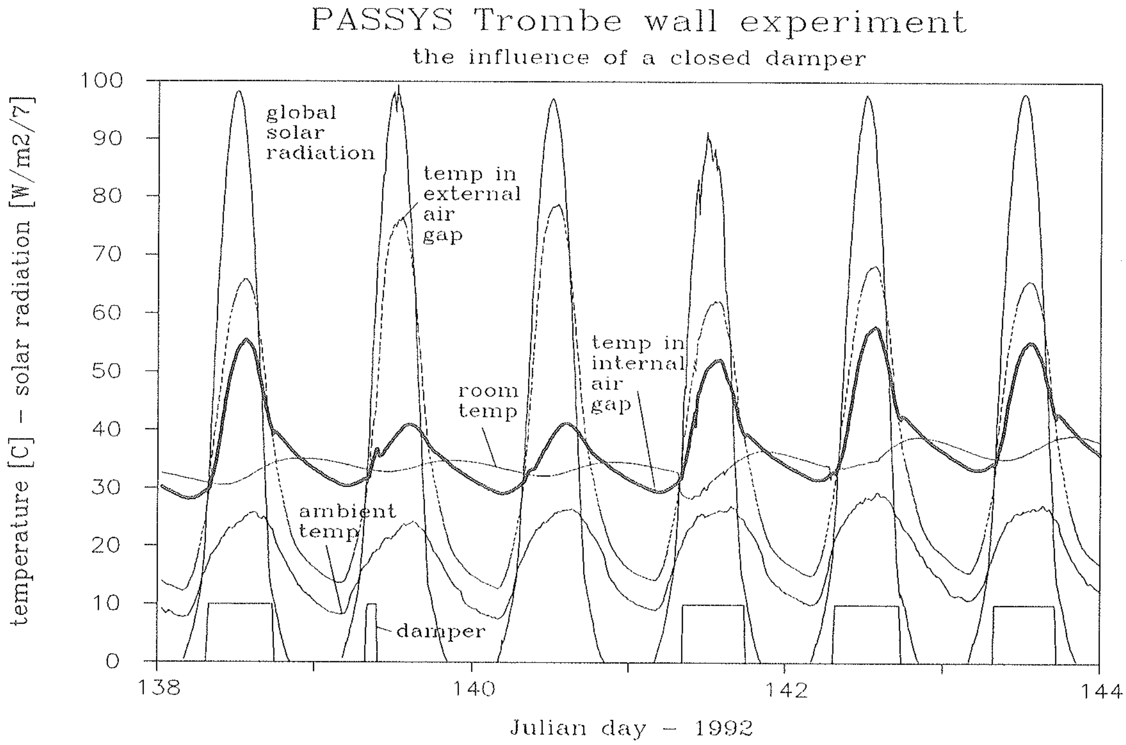

Figure 3.26 The temperature of the two air gaps of the internally ventilated Trombe wall shown in fig. 3.27 during a warm summer period with and without the damper closed. Damper open: value = 10, damper closed: value = 0.

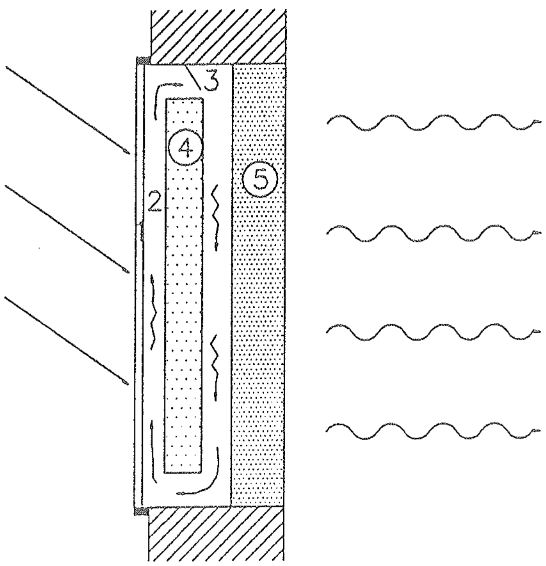

1 One layer of glass
2 Absorber
3 Motor driven damper
4 Insulation
5 Thermal mass

Figure 3.27 The internally ventilated Trombe wall tested at the Danish PASSYS test site.

4 Visual inspection of the walls

After the experiment the walls and the experimental house was left under free floating conditions for several years. It was, however, decided to demolish the experimental building in order to give room for other experiments. The experimental building was demolished in the summer of 1989 - three and a half years after the installation of the walls.

During the demolition, the constructions were inspected in order to detect any degeneration of the walls. The only detected damage was, that the bright plastic foil on the additional insulation on the thermo laths of wall 1 (see figs. 2.11-12) had lost its adhesive ability and had crumpled up.

Figure 4.1 The bright adhesive plastic foil on the additional insulation on the thermo laths of wall 1 had after three and a half years lost its adhesive ability and had crumpled up.

5 Conclusion

In Denmark it is necessary to use insulated solar walls in order to avoid losing more energy during periods without solar radiation than is gained during periods with solar radiation. The report describes the results obtained from an experiment with two insulated solar walls.

In wall 1 a blind with turnable vertical slats made of bright plastic foil was installed in the air gap between the mass component (sand/lime bricks) and the transparent cover. The blind was turnable and operated in such a way that during the day the slats of the blind were always parallel to the solar beam while the blind during the night was closed in order to decrease the heat loss from the mass component.

Wall 2 was an internally ventilated Trombe wall. An insulating panel was mounted between the mass component and the absorber. At the top and bottom of the insulating panel dampers of plastic foil and a grid were mounted allowing the solar heat absorbed on the absorber to be transported by a thermosiphonic air stream to the mass component. Discharge by a reverse air stream during the night was prevented by the dampers.

An investigation of the measured data from the two periods March 1-April 3, 1986 and April 22-May 7, 1986 showed that the solar gain was highest for wall 1 with the vertical turnable blind, but the heat loss was also highest for this wall resulting in almost identical performance for the two walls for the first period. Wall 2 had, during the second period, a 28% lower performance than wall 1. The higher performance of wall 1 is, however, not real as it led to considerably higher overheating problems for this wall than for wall 2.

It was not the aim of the project to develop computer models of the walls and simulate the annual performance of the walls installed in buildings. It is, however, expected that wall 2 (internally ventilated Trombe wall) would have a higher performance than wall 1 under Danish weather conditions. It happens because the heat loss from wall 1 is 67% higher than from wall 2. Wall 1 will thus, compared to wall 2, lose more energy during November-January (with low solar radiation) than it will gain during the rest of the heating season.

The U-value of a traditional heavy Danish wall should be below 0.35 W/m^2K according to the building code. The heat loss of wall 1 was, based on the measurements, calculated to be 0.75 W/m^2K - ie twice as large as a traditional wall but still only half the U-value of a solar wall with only a single-pane cover in front of the mass wall. The measured U-value of the wall was very close to the theoretical U-value of the wall with closed blind. The blind does, therefore, decrease both the radiative and convective heat loss - also when it is open.

The measured U-value of wall 2 was only about 30% higher than that of a traditional wall. The measured U-value of wall 2 is further very close to the theoretical U-value; it thus seems that the dampers of the insulated panel did operate as expected during periods without solar radiation, so that the mass component was not discharged due to a reverse circulation of air between the two air gaps.

The measurements show that some problems with the thermal comfort may be expected - especially overheating problems. The wall does, however, have a built-in overheating protection. If the blind of wall 1 is closed during the summer, the incoming solar radiation will be reflected out again without causing much increase of the temperature level of the wall. If manually operated dampers were installed in wall 2 and kept closed in the summer, the wall would be transformed into almost a traditional wall where the heat is no longer transferred by an air stream but only via conduction through the insulating panel.

A visual inspection during the dismantling of the walls three and a half years after the installation showed no damages of the wall except that the bright foil fastened on hard insulation had lost its adhesive ability and had crumpled up.

Based on the experience gained from the experiment it is anticipated that the walls are suitable under Danish weather conditions. More detailed investigations are, however, necessary in order to determine the annual savings of the walls installed in real buildings and in order to investigate if the walls are profitable.

6 References

[1] Solvægge - målt og beregnet (Solar walls - measured and calculated - In Danish). Lars Olsen. Thermal Insulation Laboratory, Technical University of Denmark. Report no 167. July 1985.

[2] Vinduer og energi (Windows and energy - in Danish). Lars Ravn-Jensen. Thermal Insulation Laboratory, Technical University of Denmark. Report no 55. April 1977.

[3] Transparent insulation for thermal storage walls. Lars Olsen and Casper Paludan-Müller. Thermal Insulation Laboratory, Technical University of Denmark. Report no 142. July 1983.

[4] Beregning af bygningers varmetab, (DS-418) NP-138-S (Rules for the Calculation of Heat Loss from Buildings - in Danish). Danish Society of Chemical, Civil, Electrical and Mechanical Engineers. 5th edition. Copenhagen 1986.

[5] Building Regulations 1982 (BR82) (in English). The Danish Ministry of Housing, The National Building Agency. Copenhagen 1983.

[6] PASSYS Services. Peter Wouters and Luk Vandaele (editors). Commission of the European Communities, DGXII. Brussels. 1993. EUR 15113 EN (not yet published).

[7] Description of Passive Solar Components. Alan Guy (editor). Commission of the European Communities, DGXII. Brussels. 1993. EUR 15121 (not yet published).